Materials Today Sustainability 20 (2022) 100240

Contents lists available at ScienceDirect

Materials Today Sustainability

journal homepage: https://www.journals.elsevier.com/materials-today-sustainability

3D printed geopolymer composites: A review

S. Qaidi [a, b, *], A. Yahia [c], B.A. Tayeh [d], H. Unis [e], R. Faraj [f], A. Mohammed [e]

[a] Department of Civil Engineering, College of Engineering, University of Duhok, Duhok, KR, Iraq
[b] Department of Civil Engineering, College of Engineering, Nawroz University, 42001 Duhok, Iraq
[c] Department of Civil Engineering, Université de Sherbrooke, 2500 Blvd. de L'Université, Sherbrooke, QC J1K 2R1, Canada
[d] Civil Engineering Department, Faculty of Engineering, Islamic University of Gaza, P.O. Box 108, Gaza Strip, Palestine
[e] Civil Engineering Department, College of Engineering, University of Sulaimani, Sulaimaniyah, KR, Iraq
[f] Civil Engineering Department, University of Halabja, Halabja, Kurdistan Region, Iraq

ARTICLE INFO

Article history:
Received 14 May 2022
Received in revised form
21 June 2022
Accepted 24 September 2022
Available online 10 October 2022

Keywords:
3D printed geopolymers
Concrete
Processing
Performance requirements
Mix design
Rheology
Mechanical properties
Applications
Challenges
Economic
Environmental footprints
Sustainability

ABSTRACT

The application of three-dimensional printed (3DP) technology is expected to lead to the industrial revolution 4.0, disrupting the economy and providing design customization and adaptation. The construction sector is rapidly catching up to this modern technology with the production of a 3D printer for concrete to provide a healthy work environment, economic independence, and architectural freedom. Despite the fact that 3DP concrete technology has progressed significantly in recent decades, there is an urgent need to develop appropriate 3DP materials that improve performance while reducing material consumption, which is critical for reducing carbon dioxide emissions. Geopolymers (GPs) have been found to be a promising alternative to cement-based materials for 3DP in the construction industry, which could help make it more environmentally friendly. This article comprehensively reviews the printing process, performance requirements, advantages, disadvantages, and common 3DP concrete technologies. This article also provides in-depth studies on the behaviors and characteristics of GP composites utilized in 3DP production, such as mix design, rheology, and mechanical characteristics. Besides, study developments are moving towards a comprehensive understanding of the environmental footprints and economic benefits of 3DP concrete for building applications utilizing GPs as suitable concrete materials for the emerging environmentally friendly robust concrete compound for digital constructions today. This review article also highlights knowledge gaps or potential challenges that must be overcome to progress GP composites for 3DP, as well as future study opportunities based on prior research and existing challenges.

1. Introduction

Three-dimensional printed (3DP) concrete is a type of additive manufacturing (AM) that is gaining traction in the construction sector due to its feasibility. The simplest and most commonly utilized type of 3DP concrete is extrusion-based concrete printing: a layer-by-layer concrete extrusion process that enables the fabrication of medium-to-large-scale civil engineering structures like pedestrian bridges, office buildings, single-or multistorey houses, and similar structures. Usually, and at an accelerating rate, novel demonstrations of the technique are made public. Some examples of large-scale 3DP concrete structures are shown in Fig. 1.

The primary benefits and possibilities of 3DP concrete are its capacity to create structures with minimum human intervention and sufficiently short time. Although the procedure is still more costly than traditional structures, due to the additional structural stability concerns, 3DP concrete offers a clear cost-benefit when increasing automation or complexity is demanded. Several of the earliest research publications reporting on 3DP concrete were published about a decade ago [1,2]. Numerous evaluations of 3DP concrete have been written since then, covering a range of diverse issues in this sector, comprising the field's patterns [3–5], the primary opportunities and problems [6–10], the broader idea of digitized concrete [11,12], the methods and technologies employed [13,14], and the basic physics of the extrusion of cementitious materials [15–18]. Although the accomplishments to date in achieving large-scale complex concrete buildings [19–25], the exponential growth in design complexity in constructing concrete

* Corresponding author.
E-mail address: shaker.abdal@uod.ac (S. Qaidi).

https://doi.org/10.1016/j.mtsust.2022.100240
2589-2347/

Abbreviations

AM	Additive manufacturing
CAD	Computer-aided design
DIW	Direct ink writing
ECC	Engineered, strain hardening cementitious composites
GO	Graphene oxide
PVA	polyvinyl alcohol
SCMs	Supplementary cementing materials
FA	Fly ash
GGBS or GGBFS	Ground-granulated blast-furnace slag
SHCC	Strain-hardening cement-based composites

structures deserves additional exploration and definitely offers significant potential for 3DP concrete. The forms and shapes of 3DP concrete constructions are often curved and rounded, deviating from more conventional design techniques. This is because the AM technique is not restricted to standard straight lines, but also confers a distinct advantage on AM structures in a spectrum of uses. This has already been demonstrated to be extremely beneficial in metal AM, where industrial adaptation is being driven by the capability of complexity to make lightweight components with the same strength, the capacity to consolidate component sections into a specific design, and the capacity to absorb cosmetic organic and biomimetic design elements into the sections [26–28].

On the other hand, A geopolymers (GP) are amorphous three-dimensional alumina-silicate binder materials, which were first named and developed by Davidovits in the late 1970s, generated by reacting a source material composed almost entirely of Al_2O_3 and SiO_2 (for example, metakaolin) with an alkaline medium (mostly alkali hydroxide/silicate) [29,30]. After source materials rich in Si and Al are activated by mixed alkaline solution, dissolved Si^{4+} O_4 and Al^{3+} O_4 tetrahedrons combine to form monomers by sharing one oxide atom. Monomers interact to form oligomers and then to synthesize 3D network of aluminosilicate structures. This dissolution and polycondensation process is called geopolymerization [4,12,31,32]. Fig. 2 shows in simplified form the geopolymerization process.

3DP technology and the adaptation of GPs to this innovation have lately attracted increased attention because of their meaningful impact on the building industry's sustainability strategy. While the purported benefits of the digitalized industry include improved quality, reduced building time, geometric flexibility, economic productivity, and reduced natural resource consumption [33–35], intrinsic challenges like structural stability and constructability must be solved by investigators [14,36–42]. As a result, the need to conduct a thorough literature review on the current state of GP behavior on 3DP concrete for construction applications is significant. This article comprehensively reviews the printing process, performance requirements, advantages, disadvantages, and common 3DP concrete technologies. This article also provides in-depth studies on the behaviors and characteristics of GP composites utilized in 3DP production, such as mix design, rheology, and mechanical characteristics. Besides, study developments are moving towards a comprehensive understanding of the environmental footprints and economic benefits of 3DP concrete for building applications utilizing GPs as suitable concrete materials for the emerging environmentally friendly robust concrete compound for digital constructions today. This review article also highlights knowledge gaps or potential challenges that must be overcome to progress GP composites for 3DP, as well as future study opportunities based on prior research and existing challenges.

2. Significance of the study

The purpose of this review is to investigate the influence of innovative production techniques on the performance and eco-efficiency of geopolymer composites. The researchers focused on four key aspects: (1) advantages geopolymer materials in comparison to traditional cementitious counterparts; (2) performance requirements for 3DP-geopolymers as a construction material; (3) mix design concepts; (4) rheology, mechanical, properties; (5) application and development direction of 3DP-geopolymer materials; (6) and future challenges.

Moreover, it is hoped that this review study will give an overview of all the current information about 3DP geopolymer and encourage its use in building infrastructure. In addition, the review forms a basis for further research on this substance and describing research insights, existent gaps, and future research directions.

3. Three-dimensional printing technology

3.1. Printing process

3.1.1. Additive manufacturing process

In construction, additive manufacturing (AM) processes are classified into two main types, as shown in Fig. 3, depending on their performance parameters [46]: (1) powder-based technique, which is eligible for producing extremely complex structures with high accuracy. Concrete layers are constructed using this approach by introducing liquid binder onto the powdered beds, especially along the chosen path given by the computer-aided design (CAD) model to retain the powder particles safely. After finishing, surplus binder powder is scraped from the build platform to produce the component geometry [47]. Powder printing is a method for producing small-scale and complex building elements like panels, interior structures, and permanent formwork that can be fitted when printing is completed [48]. Powdered printing techniques like emerging objects [49,50] and the D-shape approach [51,52] are examples; (2) extrusion-based technique, which is the most extensively utilized 3DP technology, where concrete materials are extruded sequentially from a nozzle placed on a pedestal. Extrusion-based techniques are commonly used on the Jobsite for structural applications such as large-scale architectural components with complex geometry. Extrusion-based- techniques of 3DP processes are classified into: concrete printing [53] and contour crafting [54–56]. Furthermore, the RILEM Technical Committee 276 `Digital fabrication with cement-based materials´ [15] stated the following explanations and statements: three main categories of extrusion-based three-dimensional concrete printing (3DCP) are identified as: (1) extrusion of stiff material, similar to conventional extrusion; (2) extrusion of flowable material with or without addition of admixture(s) in the printhead, and (3) extrusion of material using additional energy input, e.g. vibration to facilitate delivery and deposition of stiff mixtures. To each category and each production step, i.e. transportation of build material, printhead process, deformation of build material during deposition, and behavior of build material after deposition, relevant processes and corresponding physical fundamental are presented [57].

3.1.2. Printing process for 3DP concrete

According to Wang, Shen [59], the printing processes for 3DP concrete mixes are divided into three steps, as illustrated in Fig. 4: (1) G Code generation; (2) material preparation and transport to the printer; and (3) printing step. To begin, a 3D model is created using

Fig. 1. Recent examples of large-scale 3DP concrete structures [43,44].

any computer-aided design application. The developed model is generated as a stereolithography (STL) format, which is a widely used format in the 3DP sector. The 3D model is then processed using any slice process to make G Code. Passing the resulting G code to memory completes the model generation process. The next step is to prepare cement-based material ingredients for printing. While the ingredients are being prepped, the printing process takes place, utilizing the hopper-pump-nozzle system illustrated in Fig. 5. Printing the building created in the computer-aided design application completes the procedure [60].

3.2. Performance requirements for 3DP-concrete

3DP technology has gained substantial attention in the building sector over the last several years due to its cost-efficiency and rapid building speed [63,64]. Additionally, it has the ability to fundamentally alter conventional construction techniques through the use of technology and digital modeling to create free-standing structural components [65,66]. The 3DP process is categorized into four stages: pumping, extrusion, building, and strength development. Thus, to fulfill printing criteria, 3DP substances must have high rheological and mechanical characteristics. Below is a specific analysis of the characteristics:

(1) Process of pumping and extrusion (suitable extrudability). Extrudability is enhanced by the pumping and extrusion processes. Extrudability is defined as the ability of a material to flow smoothly via an extruder without fouling or disrupting the piping flow, in other words, the capacity to extrude the mixture via a nozzle with a minimum level of

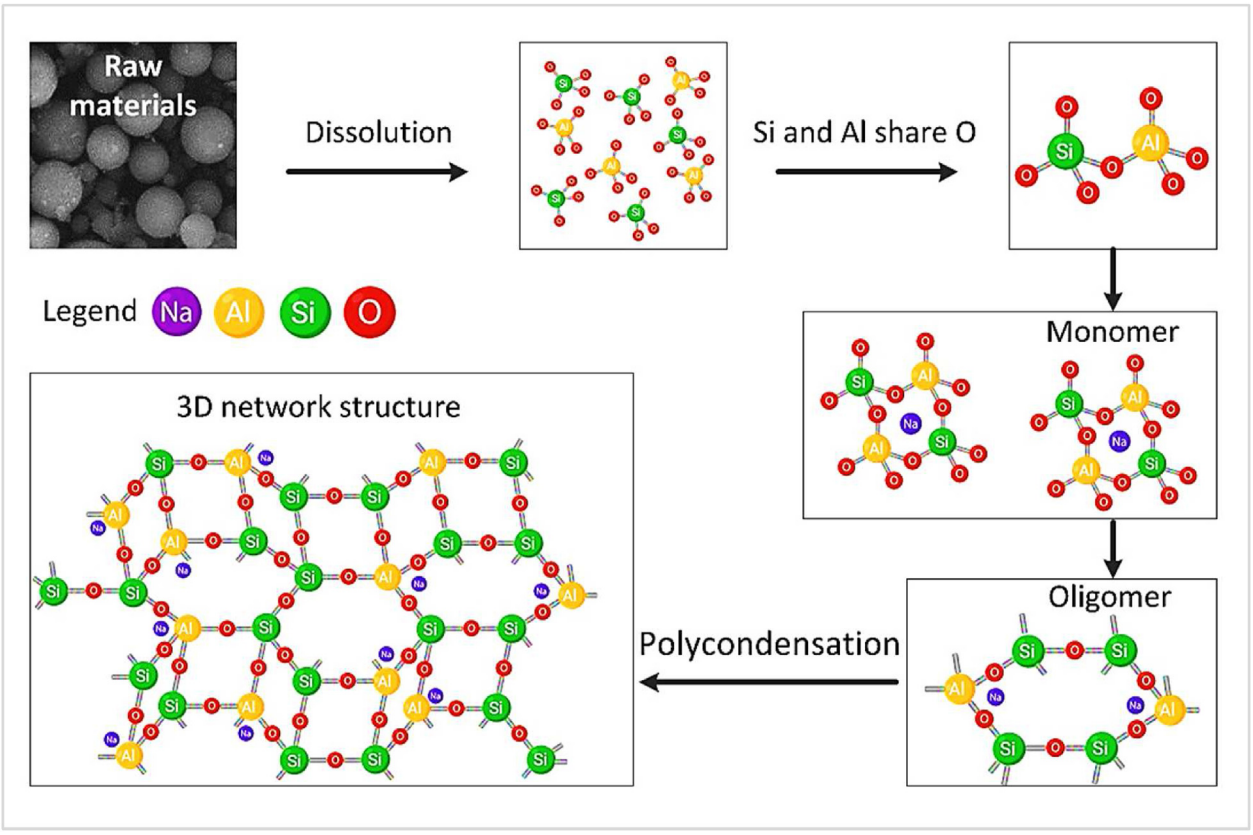

Fig. 2. Simplified geopolymerization process [45].

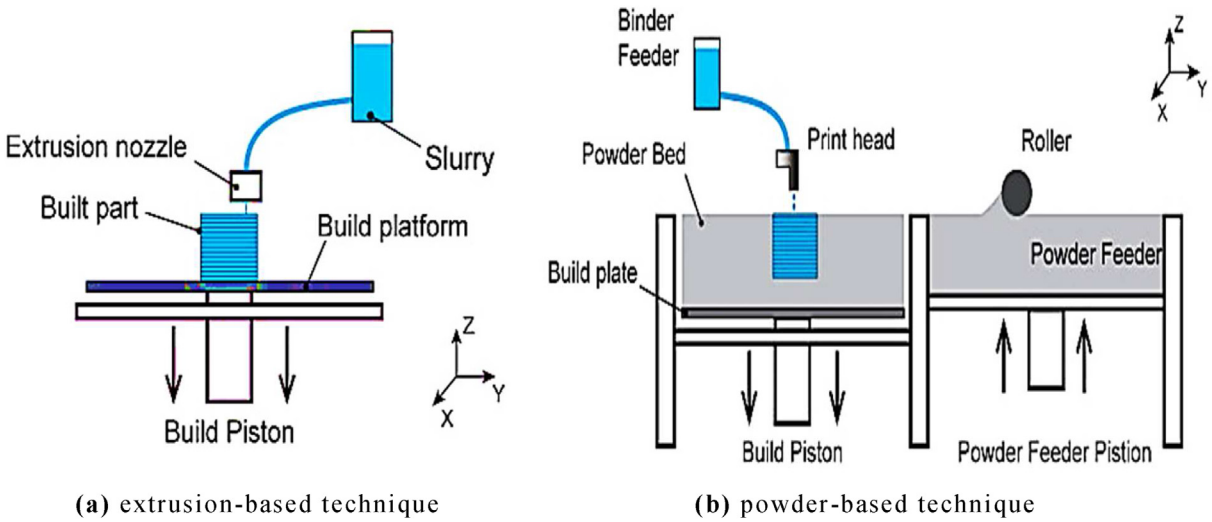

Fig. 3. A diagram of the additive manufacturing technique [58].

filament tearing/splitting and without significant cross-sectional deformation. Fig. 6 (extrusion using a 40 × 10 mm rectangular nozzle) and Fig. 7 (diagram of an extrusion-based 3DP, the concrete filament is pushed across the extruder and placed on the substrate layer-by-layer) provide examples. The 3DP construction material should be pumped via pipe and extrudable by an extruder head; consequently, it cannot be too thick to choke the pipes during pipeline transit [66–68]. Moreover, when the concrete mix is pumped, it segregates in the hose pipe, generating a lubricating layer that contributes to pump pressure drop [69]. This lubricating layer forms due to shear-induced particle migration, which occurs when aggregate migrates away from areas of high shear stress. The velocity distribution along the pipe's cross-section, as described by Kwon, Jang [70] and illustrated in Fig. 8, demonstrates that the majority of the velocity is created in the lubricating layers observed near the wall. Nevertheless, uncontrolled segregation can result in a

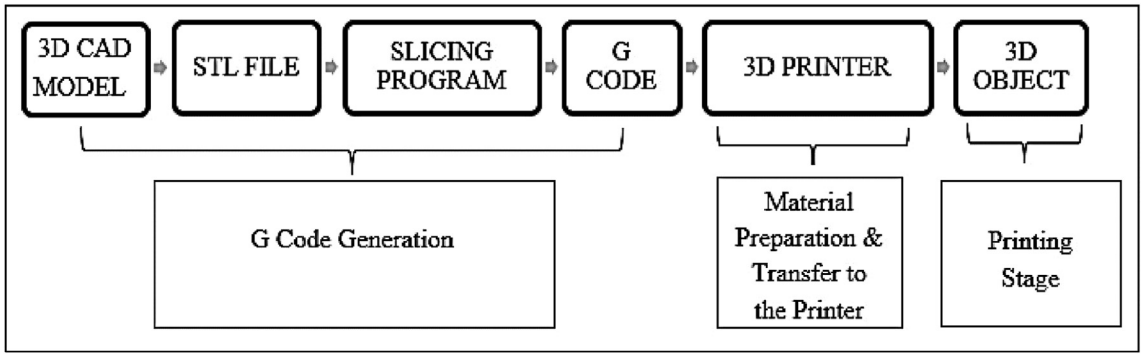

Fig. 4. General work flow for 3DP concrete [61].

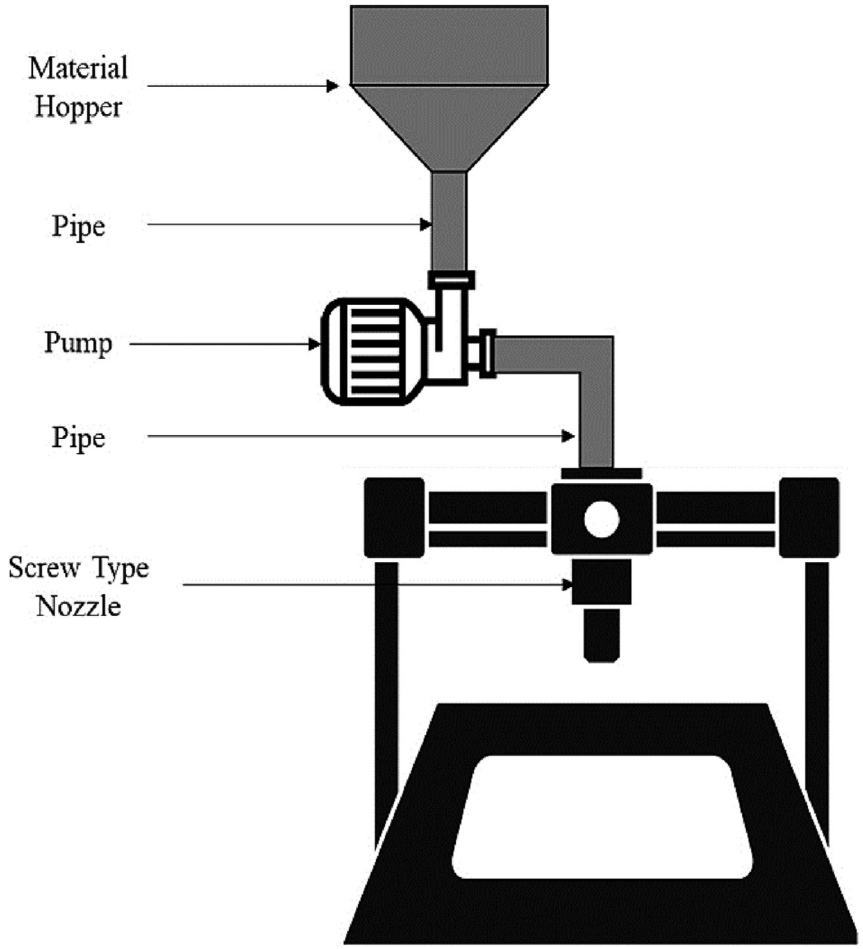

Fig. 5. Hopper-pump-nozzle system [61,62].

low-quality filament extruded from the mixture. This could affect the printed specimen's hardened characteristics. Since most of the lubricating layer will be pasted, shrinkage fractures may happen, making the printed concrete less durable.

(2) the construction process (good thixotropic properties and form retention). Following extrusion, the material should preserve its form according to the extruder dimensions during the building process, which may be quantified using a dimensionless value termed the shape retention factor. Additionally, the material must regain its original viscosity to support the load imposed by succeeding layers, and a dimensionless factor is utilized as the thixotropy index. Fig. 9 presents the conflicting rheological parameters for the 3DP concrete process, including pumpability, extrudability and buildability for workability requirements, and low dynamic yield stress and high static yield stress for rheological requirements. Moreover, According to Bos, Kruger [71], the material characteristics of the applied print mortar are an important parameter to determine buildability. However, it is not yet clear which material properties are the most suitable, and how they should be determined experimentally [71].

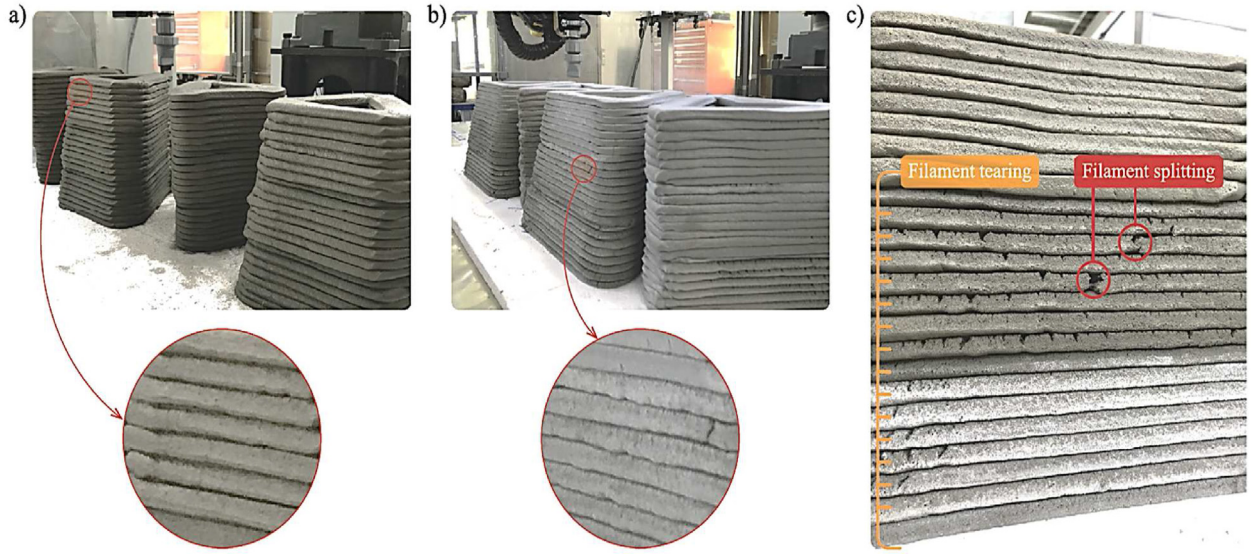

Fig. 6. Extrusion using a 40 × 10 mm rectangular nozzle: a) good-quality concrete filaments without indications of tear, b) concrete filaments with indications of tearing throughout extrusion due to a lack of paste content, and c) concrete filaments tearing in layers 1–16 and splitting into layers 12 and 13 [75].

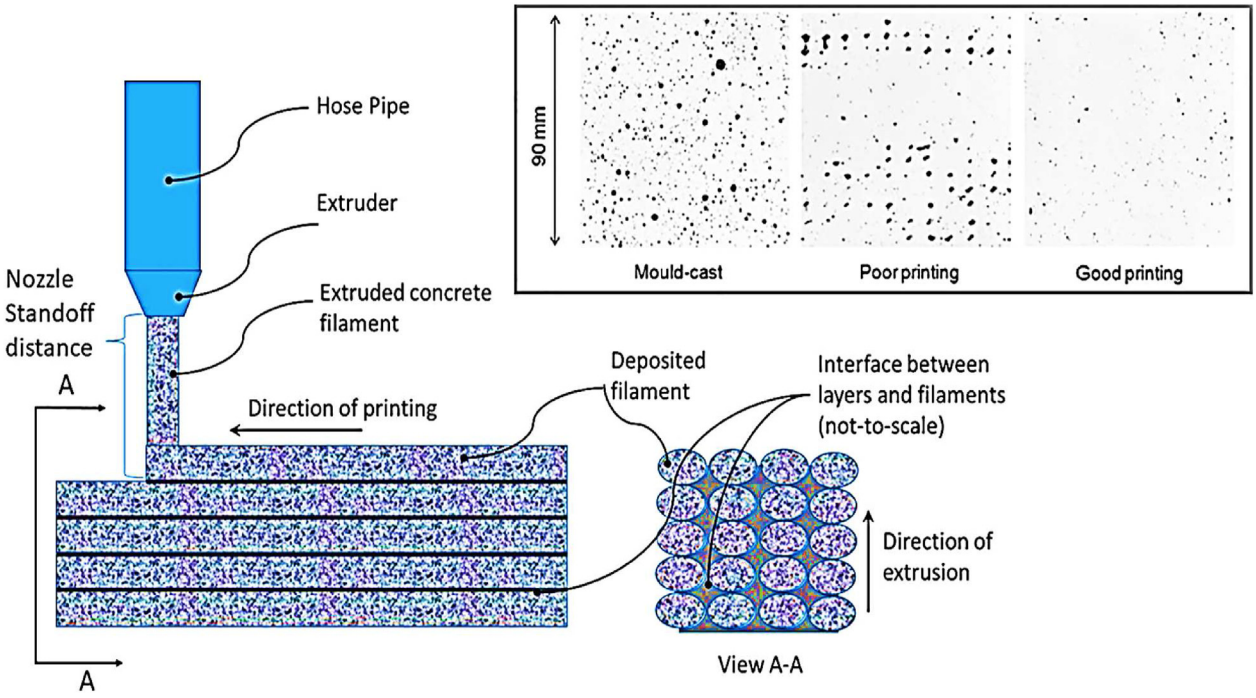

Fig. 7. Diagram of an extrusion-based 3DP; the concrete filament is pushed across the extruder and placed on the substrate layer-by-layer. Due to its own weight and the weight of the layers above it, the deposited filament deforms [2,76].

(3) The process of developing strength (sufficient bond, compressive and flexural strengths). Finally, the 3DP construction material must possess sufficient bond strength and early strength to be stable under the pressure of later layers [72,73]. However, as with any structure, enough compressive strength and flexural strength are required.

The low early strength and prolonged setting time of ordinary Portland cement (OPC) have restricted its use as a 3DP material. In comparison, GP materials have immense promise as 3DP construction materials because of their greater early strength and condensation rate [74]. Additionally, as a novel form of green gels substance, GP has garnered considerable interest from the building sector because of its energy and environmental-saving benefits when compared to OPC's high-power consumption. Several researchers have conducted pertinent research on it to can be employed as a sustainable and environmental material in 3DP structures.

3.3. Advantages and disadvantages of 3DP technology in construction

Digital fabrication techniques with concrete and cementitious materials have witnessed a large volume of research and industrial

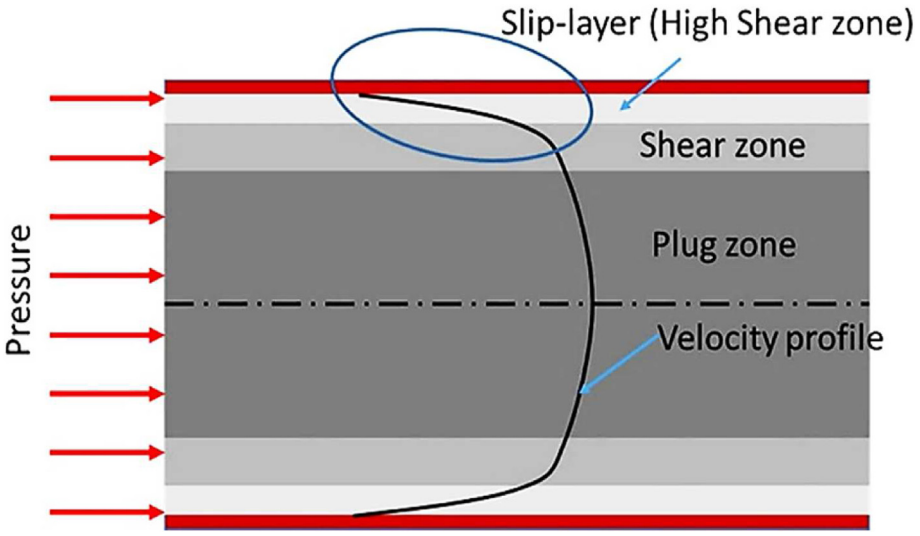

Fig. 8. The profile of velocity along the cross-section of a pipe carrying concrete [70,76].

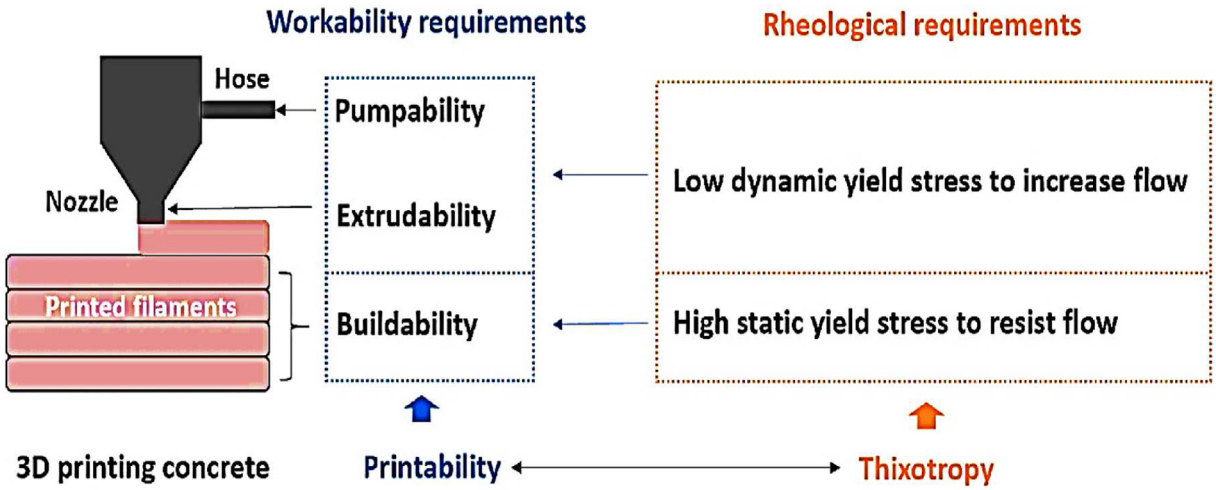

Fig. 9. Conflicting rheological requirements of the process concerned in 3DP concrete [77].

activity recently, with industrialization of techniques such as 3D printing becoming more of a reality. The potential to revolutionize construction is real, not only through reducing costs, but also bringing more sustainability and increased functionality [11,78]. Material challenges are significant, chief among them being understanding and controlling early age hydration and the link to rheology, incorporation of reinforcement, and overall, the link between processing, material, and performance, both from a structural and durability point of view. Interdisciplinarity is crucial, as the field brings together many disparate fields and has been driven by fields such as architecture so far [11].

According to the developers, 3DP technology offers several advantages over conventional methods employed in concrete technology, including the ability to speed up production, reduce accidents in the workplace, reduce waste of materials, and partially reduce costs [43,75,79–86]. One of the most significant advantages of 3DP technologies is the cost savings associated with formwork [81,87–89]. Formwork can contribute to a sizable portion of the overall cost of concrete construction [90–95]. Additionally, the use of formwork in concrete manufacturing results in building delays, severe negative environmental impacts, and expensive labor and material costs. As a result of these advantages, demand for 3DP technology continues to grow. Nevertheless, investigations into the application of 3DP printers in construction manufacturing are still in their early stages. It was established that there are no applicable standards, design specifications, or processes [22,96,97]. This was seen as a disadvantage since it makes identifying an optimal mix design for 3DP concrete fairly difficult. It was noted that 3DP concrete mixes should have the distinct fresh condition and rheological characteristics of ordinary concrete to enable buildability [71,98–100]. Additionally, 3DP concrete mixes have less fluidity than self-compacting concrete (SCC)/ordinary concrete [101–103]. As stated by Le, Austin [104], the characteristics of 3DP concrete mixtures are a combination of shotcrete and self-compacting characteristics.

3DP concrete mixes must exhibit distinct rheological characteristics during and after extrusion, as stated by Souza, Ferreira [105]. To enable the printing of mixes, materials must be readily flowable from the blender to the nozzles. On the other side, to enable continuous extrusion, mixes must have a low viscosity and

low yield stress. Moreover, it was claimed that the mixes should have a high viscosity and a high yield-stress value to enable layer-by-layer construction, bear the weight of the top layers for every layer, and avoid deformation, [73,106,107]. Research has indicated that viscosity modifying agents and nanoclay are frequently employed to achieve the appropriate rheological properties in 3DP concrete [108]. As is well documented, a significant proportion of cement is utilized to provide printability to 3DP concrete mixes [76]. Increased cement content results in an increase in the hydration heat [109]. This might lead to higher drying shrinkage and nozzle blockage. When less cement is applied, various drawbacks include prolonged setting time, low early strength, and crack development [110]. As a result, studies recommend the use of mineral additions in 3DP concrete mixes. Additionally, the absence of coarse aggregate due to the tiny nozzle diameter is considered to have a serious danger of drying shrinkage. Investigators advised that fiber be added to 3DP concrete mixes to lessen the possibility of drying shrinkage [111–114]. Recently, a certain type of geopolymer composite appeared which attracted the attention of researchers; It is the use of plant fibers. This new compound needs more attention in future studies on the opportunity to exploit it in 3D printing [115–117]. In addition to what was mentioned above, Fig. 10 presents more advantages and disadvantages of a 3D printer.

3.4. Economic prospects of 3DP concrete technology

The economic benefits of 3DP concrete are not readily evident in large-scale construction, but the increased geometrical flexibility provided by this innovation alone provides significant advantages. This geometrical flexibility enables the developers to design ideal topological structures and minimizes the possibility of utilizing materials that are not permitted under standard construction processes [118,119]. Additionally, significant economic advantages may be realized as a result of the lack of coating. Moreover, the development of new building materials based on alkaline activation technology is very promising, mainly linked to products that need significant technological properties and durability due to their adverse service conditions and environmental exposure [120]. In general, 3DP concrete can reduce the costs of building by 25% in comparison to precast buildings, owing to the lack of form [90]. As shown in Fig. 11, the cost distribution of various activities within a typical construction project approaches 50%, with labor and formwork costs contributing to more than half of the total cost [121]. Nevertheless, the cost of the machines and materials may be greater than in traditional construction. Moreover, the economic consequences of a wall constructed with 3DP concrete against a traditional process were investigated [122]. In general, 3DP concrete is more efficient and productive than conventionally produced structures, particularly those that are more complicated.

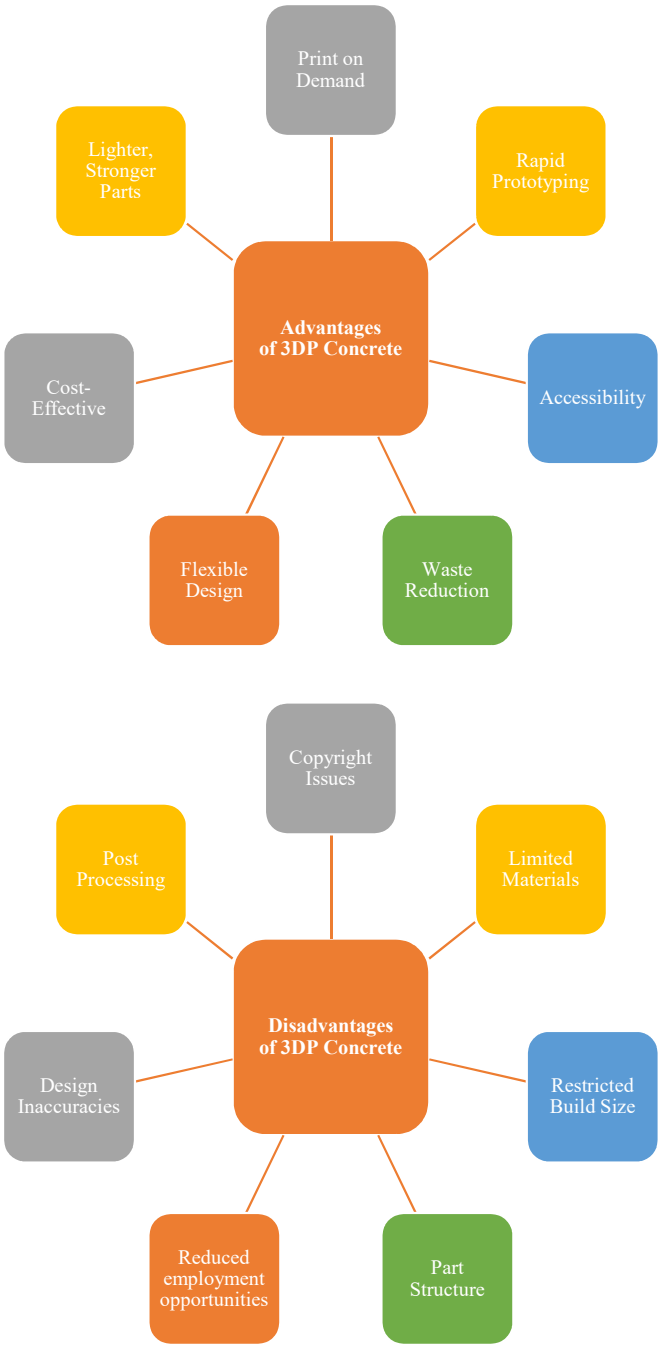

Fig. 10. Advantages and disadvantages of 3DP-concrete technology [43].

3.5. Application and development direction of 3DP concrete

Trial projects are now being realized at an increasing rate around the world to test the viability of the technology against real-world requirements. This step, from the 'simple' deposition of filaments of self-stable concrete to its application in buildings and structures, with all associated requirements and interfaces, comes with challenges [57,78,123]. In many of these areas, much simply remains unknown due to a lack of experimental data or information from projects where 3DCP has been applied. Bos, Menna [123] aimed to narrow this knowledge gap by providing a systematic discussion, based on the analyses of eight realized 3DCP projects from around the world. It was found that the structural application of printed concrete is limited, due to a lack of regulatory framework for expedient approval, as well as limited reinforcement options which require to resort to unreinforced masonry analogies. The application of the technology features a host of practical issues that relate to the print process, material, site conditions, building integration and design – or to the 3DCP technology in general. Although some potential risks, such as shrinkage cracking and quality consistency are generally recognized, the measures taken to mitigate them vary considerably, and are largely based on individual expertise. The actual effectiveness is generally unknown. Finally, it was observed that, while the printing itself is fast, the preparation time is generally considerable. This is partially due to a lack of knowledge amongst professionals. In the practical production of a 3DCP project, three expertise areas are crucial: one for the digital part, one for the machine side, and one for the material side.

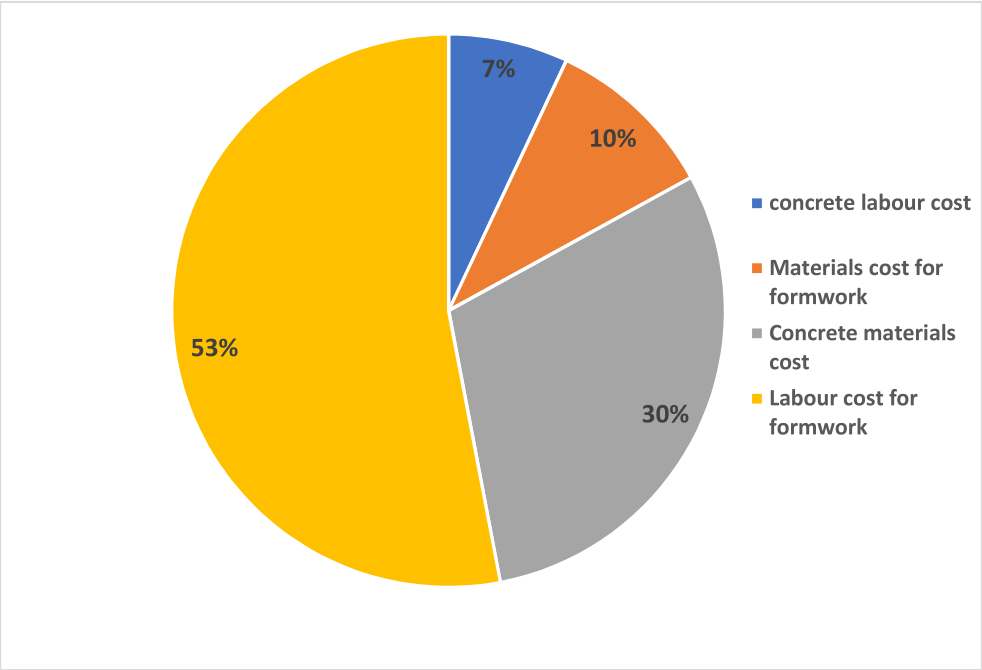

Fig. 11. Cost distribution for a typical construction project [121].

Thus, there is a strong need for educational institutions to develop dedicated training courses and incorporate relevant topics into their curricula.

Robotic and automation technology are more required in high-rise structures owing to the requirement to minimize human resource needs, building complexity, and safety issues associated with high-rise structures [124]. The expenditures on structural construction equipment and maintenance also increase as the size of non-structural and structural elements increases [125]. Large organizations that are primarily involved in structural applications can invest in developing robotics eligible of handling high-risk, complicated structural components. In comparison, deploying robotic technology is a problem for small- and medium-sized businesses that specialize in making small, customized buildings [126,127].

3DP concrete applications are classified into two categories: small-scale 3DP concrete and large scale 3DP concrete. After obtaining appropriate dimensions, blending, and designing materials, key printing characteristics, and fundamental geometries like circular columns, prisms, and cubes small-scale 3DP concrete models are simply printed. By comparison, broad 3DP is a highly specialized kind of AM that focuses on the fabrication of big, huge, and frequently permanent buildings or structures. As a result, specialist firms with exceptional capabilities are required to apply this sort of 3DP for structures [98,128,129].

The public's interest in large-scale 3DP was piqued by a Chinese organization called Yingchuang, which claimed to be able to print ten full-sized houses per day for less than $5000 per house using a top-secret cement mixture made entirely of recyclable materials. Yingchuang utilized contour crafting, a technique pioneered by experts at South California University [130]. Irrespective of Yingchuang's dependability, the organization was clearly successful in generating a hot zone for large-scale 3DP and convincing countries to fund it. Subsequent to that enthusiasm, the Egyptian government contracted with Yingchuang to print twenty thousand solitary housing units, the U.A.E. government contracted with Yingchuang to print the office of the future and Saudi Arabia officials recently discussed the utilization of 3DP to create a million and a half housing units with Yingchuang.

Furthermore, the criteria for printability in large-scale 3DP concrete may change from what is in research lab 3DP concrete, since a larger volume of concrete is made, transported, stored, supplied, and printed in real buildings. Just a few investigations have investigated the printability criteria for 3DP concrete at the laboratory and field scales [131]. Table 1 highlights the several parameters of field-and laboratory-scale 3DP concrete, including the size of nozzles, pumping range, the size of filaments, and the size of a single printed layer.

As mentioned earlier, when the silicon dioxide/sodium oxide [SiO_2/Na_2O] ratio of the alkali-activator sol is 3.22, the resulting geopolymer (GP) exhibits acceptable strength, acceptable expansibility and workability, and a good capacity for shape retention [132]. Moreover, the compressive strength of 3DP-geopolymer concrete made with 50% fly ash (FA) and 50% ground-granulated blast-furnace slag (GGBFS) is 25 MPa, which is satisfactory for a broad range of sectors [133]. Besides, by directly adding 1.2 mm continuous micro-wire ropes into GP composites after the filaments of 12 mm were deposited, the mechanical strength, toughness, and deformation of GP composites subsequent to cracking were greatly enhanced [10,134]. In addition, by introducing 0.4% nanoclay to the GP, the thixotropic characteristics of alkali-activated GGBFS were enhanced, and by including 2% of water graphite seedlings in this hybrid system, hydration is improved and, as a consequence, the structural accumulating rate demanded large-scale 3DP is increased.

4. Mix design concepts

4.1. Mix design parameter

Recent progress in robotics and automation for the building and construction sector has prompted huge attention to the use of AM and 3DP to produce building materials, full scale buildings, and modular components of construction [143]. From design through

Table 1
Description of a single-large-scale printed layer including several types of 3DP concrete.

Section	Nozzle size, ⌀ (mm)	Pumping distance (mm)	Width x filament height, (mm^2)	Printed single layer size, length (mm)	Refs
Laboratory- scale 3DP concrete	8 × 24 mm^2	–	30 × 8	2000	[135]
	30, circular	–	30 × 10	Ø 300 mm cylinder	[136]
	20, circular	–	35 × 15	1350	[137]
Section fabricated beforehand of 3DP concrete	10, circular	5	10 × 11	1860 × 460 mm^2 curved wall	[138]
	60 × 10 mm^2	10	60 × 12	25 and 100	[139]
	25, circular	–	25 × 20	3000 × 450 mm^2 beam	[140]
Monolithic 3DP concrete	150 × 150 mm^2	18	150 × 50	4600 × 12,100 mm^2	[141]
	38, circular	15.2	38 × 25	60,000	[142]
	40 × 40 mm^2	1000 × 20,000 mm^2	60 × 30	greater than 30	

production, 3DP technology has great promise for conserving natural resources and lowering construction costs and time [33]. Nevertheless, various obstacles, ranging from mixed proportion to the strength and durability characteristics of the printing materials, must be addressed to effectively manufacture these products. Along with the inherent issues associated with 3DP production, like anisotropic behavior and structural integrity, newly emerging properties like buildability, interlayer bonding capability, printability must be taken into consideration when designing an appropriate mix proportion of these components.

Because 3DP concrete is categorized as unique concrete, it was assumed that they were designed without acceptance criteria, standards, or guidelines. As previously stated, current standards do not offer instructions on the design mix of 3DP concrete due to its rheological characteristics being different from ordinary concrete [144–147]. Table 2 summarizes design samples for 3DP concrete mixes discovered by many researchers. The researchers often utilize many trial mixes before arriving at the optimal design mix, as shown in Fig. 12.

Motivated by a desire to produce printable mixes with two conflicting characteristics, slump-less at rest and self-leveling under compression, the mix design of printable mixes is seldom possible concurrently [65,148]. A Casson plastic has a decreasing viscosity as the shear strain rate rises, and a threshold yield-stress acceptably reflects the required rheological model of printed mixes [149–151]. While, thixotropy is another phrase that is frequently utilized to describe Bingham composites that behave rigidly at low stresses but become viscous under high stresses, as shown in Fig. 13. Thixotropy characterizes the capacity of concrete materials to build-up and can be practically measured by the integral of the hysteresis area among the upper and lower bounds of the flow curve, as illustrated in Fig. 14. Additionally, it can be characterized as an increase in yield stress over time [152]. Therefore, combining the Bingham model and the thixotropic behavior in the appropriate rheological behavior enables simpler extrusion under compression and layer form integrity under the weight of superimposed layers and its own weight [153–155]. Owing to higher viscosity and reduced shear stress as shown in Fig. 14, GPs are often regarded as more difficult to print than their cementitious counterparts [65,156]. As a result, the 3DP manufacture of GP and alkali-activated materials requires enhancements to their adaptability and rheological characteristics.

It is worth noting that the effect of print factors on the hardened or interface characteristics are dependent on the materials mixture. Moreover, the design mixture affects the rheological properties of concrete, which includes the percentage by volume of binding compounds; aggregate properties, which include size, shape, and particle distribution; and the composition, which comprises the inclusion of GPs. Besides, chemical additives have the potential to be a very efficient way of adjusting rheological behavior. As the addition of thixotropic additives to 3DP concrete boosts its yield strength without affecting the rate of hydration of cement in the initial stages [157]. Owing to colloidal particle flocculation and continual nucleation, the thixotropy property of printed materials manifests itself in OPC-based GPs [154]. After the thixotropic material has been produced by optimal mix design, it may be adjusted by varying the admixture mixtures with the rate of a structural component (i.e. hardening) [152].

Panda and Tan [65] produced GP mixtures for concrete printing by changing the sand concentration. The binder was composed of a combination of GGBFS, fly ash and silica fume with FA contributing approximately 70% of the weight. A commercial K_2SiO_3 sol was

Table 2
Mixing of materials for 3DP-geopolymers.

Composites (kg/m^3)				Activator (kg/m^3)	Water/binder ratio	Additives: Superplasticizer & retarder	Sand	Maximum size of sand	Fibers	Nozzle size (mm)	Refs.
Cement	Fly ash	GGBFS	Silica fume								
_	100	–	–	Na(SiO3)-26Na(OH)-26	–	–	200	0.3	Steel (1%); Polycarbonate (0.5%)	–	[160]
375–643	102–184	–	54–92	–	0.26–0.44	1% and 0.5% by weight of binder	–	2	Polypropylene	9	[104]
1000	20	–	20	–	0.35	–	1000	1	–	20	[161]
1000	1000	–	100	–	0.15	1.3 g/L	500	1.2	–	30 × 15	[162]
_	573	36	102	K_2SiO_3 = 140.8	0.203	–	1220	–	–	–	[163]
_	646	39	78	KOH = 23; K_2SiO_3 = 250	0.08	bentonite: 8 kg/m^3, Actigel: 8 kg/m^3	1168	–	–	–	[153]
295	277	–	145	–	0.4	Sodium lignosulfonate: 7 kg/m^3	1211	1	0–13.5	–	
626	–	–	–	–	0.42	PC based solution 0.75%	1391	2	–	–	[164]
392	213	–	213	–	0.42	PC based solution 2%	1260	–	–	–	
_	673–546	119–96	66–54	355–289	0.08–0.063	–	869–1221	2	–		[65]

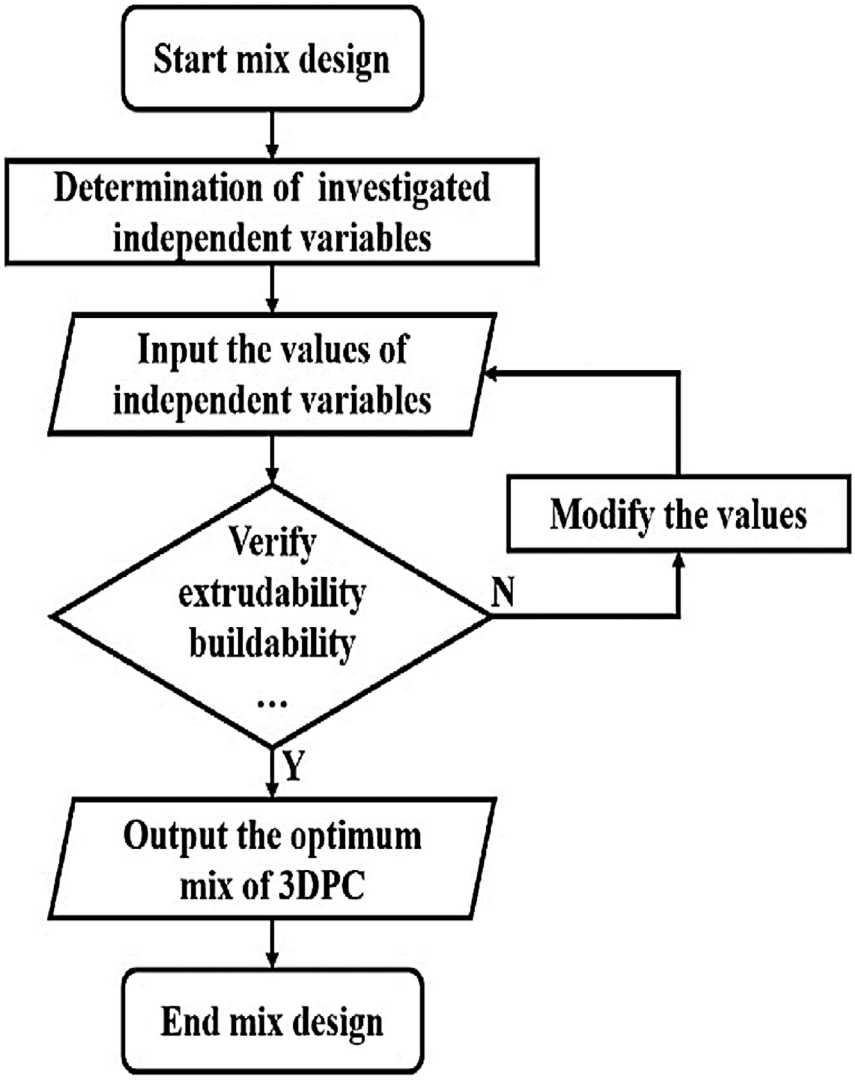

Fig. 12. The flow chart of the trial and error method [77].

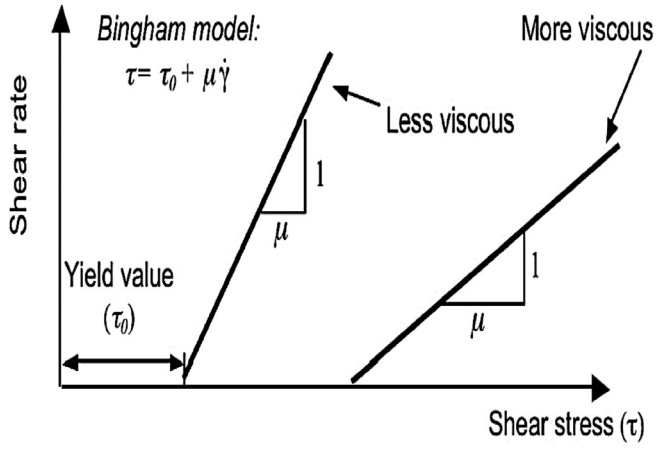

Fig. 13. A graphical representation of the Bingham model [158,159].

mixed with 18.71% Na2O, 45.0% Na(OH), and 24.32% SiO_2 sol to make the alkaline sol. To get design mixtures G-G5 with a goal strength of 25 MPa, fine sand was introduced in the binder mass ratio of 1.1–1.9. G5 and G4 mixtures with a large proportion of sand were not extrudable. Owing to the relatively short recovery period of GP mixtures throughout construction, nanoclay was introduced to the mixture G3. Moreover, in order to print the desired height of 60 cm, the yield strength of the G3 mixture has to be enhanced, which was achieved by introducing microfibers. Besides, the yield stress range of 600–1000 Pa was shown to be acceptable for the GP mixture's extrudability. According to the specification, the geometry stability coefficient should be between 0.85 and 0.90. Additionally, 10–15 min of printing time has been observed to be sufficient. Similarly, printing concrete, when it is still fresh, improves the interface bond strength of the printed layers. This is frequently complicated by the intricacy and scale of the intended shape. Fig. 15 presents a contour plot of the mix demonstrating the influence of the fly ash (FA), ground-granulated blast-furnace slag (GGBFS), and silica fume (SF) concentrations on the initial yield response.

4.2. Sustainability of 3DP-concrete mix

Table 3 summarizes the amounts of various printed concrete used in various combinations, and information on the components'

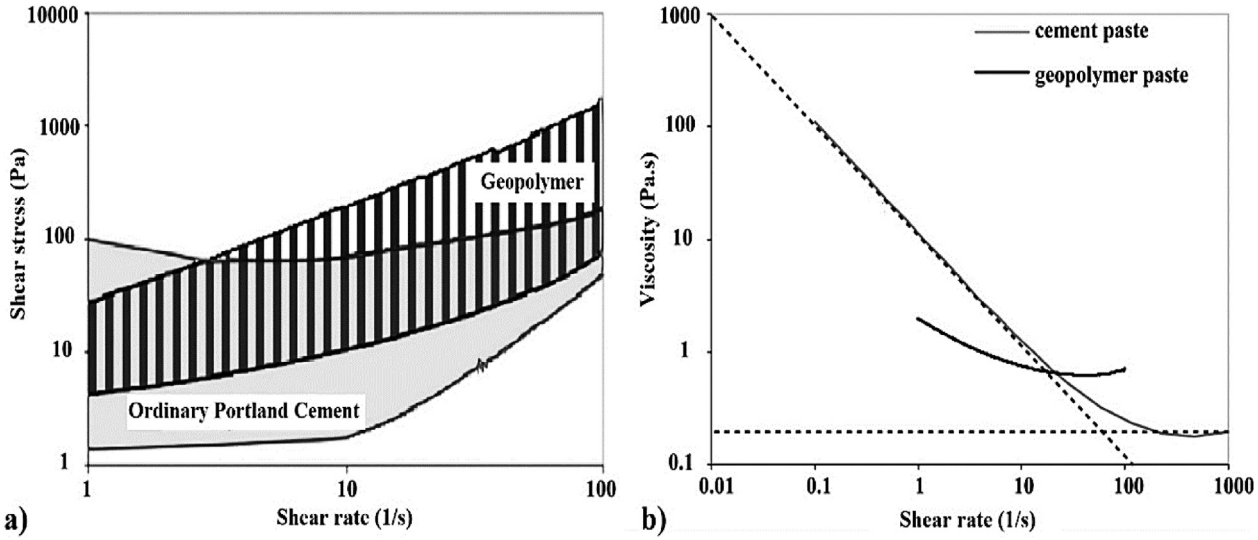

Fig. 14. Difference between (a) shear stress, and (b) viscosity vs. shear rate for cement and geopolymer pastes [156].

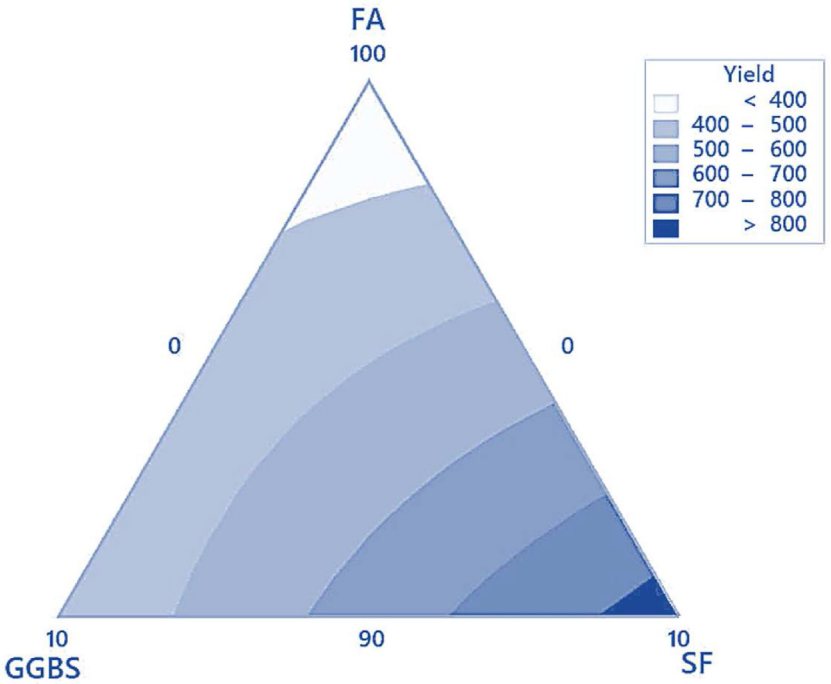

Fig. 15. A contour plot of the mix illustrates the influence of the FA, GGBS, and SF concentrations on the initial yield response [66].

Table 3
As previously published, different mix ratios of 3DP concrete and their associated CO_2 emissions.

Ingredients	3DP OPC mixture (kg/m^3) [153]	3DP-geopolymers mixture (kg/m^3) [176]	Embodied energy (MJ/kg)	CO_2 emissions (kg/kg)	Refs.
Ordinary Portland Cement (OPC)	290	–	4.8	0.85	[177]
Silica sand	1211	1090.7	0.175	0.026	[165]
Ground-granulated blast-furnace slag (GGBS)	–	363.6	0.33	0.0265	[178]
Silica fume (SF)	145	–	0.10	0.014	[167]
Fly ash (FA)	278	363.6	0.05	0.0196	[166]
Solid activator	–	72.7	17.90	0.93	[179]
Retarder	–	3.6	0.822	0.307	[180]
Superplasticizer	7	–	36.76	1.48	[165]
Water	285	261.8	–	–	[176]

life cycle inventories, as cited in the prior studies [153,165–167]. 3DP concrete has several potentials for constructing complex shapes with structural optimization [118]. This characteristic offers a more effective design by allocating the material where it is structurally necessary [119,168]. Utilizing high-performance concrete [169] in conjunction with 3DP concrete may lead to a 50% decrease in impact on the environment compared to typical structural buildings.

Digital fabrication may potentially result in significant material efficiency as a result of structural integrations and hybridizations [170]. Numerous studies have indicated that integrations and hybridizations of this type improve thermal comfort and reduce energy consumption [171,172]. Another factor to consider is the environmental impact of scaffold and formwork; in comparison to conventional concrete, 3DP concrete has a reduced environmental impact due to the absence of scaffolding and formwork. Nevertheless, since scaffolding and formwork may be reused in several construction works, their impact on the costs and environment in conventional construction can also be minimized [147,173–175].

Fig. 16 illustrates the energy consumption and carbon dioxide emissions associated with the production of offset printing concrete [176]. When specific ingredients' environmental footprints

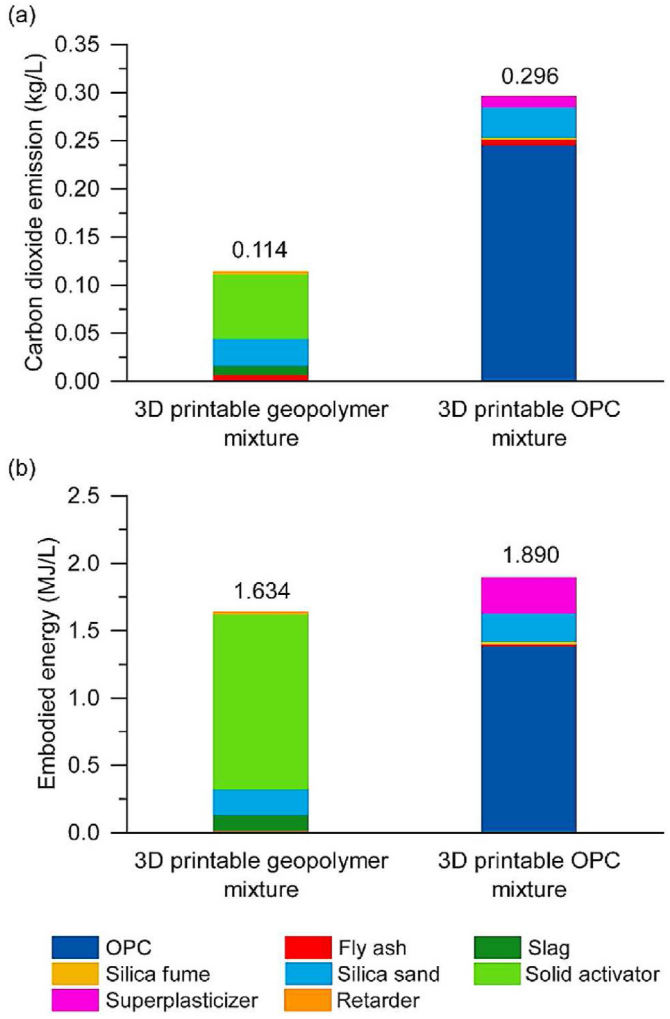

Fig. 16. (a) Carbon dioxide emissions and (b) energy content are involved in the production of the optimal 3DP-geopolymer mixtures developed in the work of Bong, Xia [176], as compared to a 3DP-OPC-based mixture with equivalent compressive strength.

are considered, the solid activator is the primary contributor in the case of GP concrete mixtures, responsible for roughly 82% of overall embedded energy and 60% of CO_2 emissions related to the production of 3DP-geopolymer concrete mixtures. In the case of an ordinary Portland cement (OPC) mix, OPC is the dominant contributor, responsible for 75% of overall embedded energy and 86% of CO_2 emissions associated with the fabrication of the 3DP OPC mix.

It is worth noting that the construction of complicated concrete buildings using 3DP concrete frequently requires a high amount of cement, as shown in Fig. 17. Printable blend designs frequently contain a larger proportion of composite and fine aggregate than standard concrete mixtures. The researchers expect that new formulas with suitable supplementary cementitious materials (SCMs) and admixtures will be created to accomplish the rapid setting needed for 3DP concrete in the coming years. Şahin and Mardani-Aghabaglou [61] demonstrated 3DP of GP using a high proportion of alkali-activators and fly ash while maintaining the required early strength. Additional studies are required in this area to determine how to enhance the SCM response at an early-age in order to compensate for early-age mechanical strength losses. Moreover, additional strategies to increase aggregate volumes and provisions for coarse aggregate inclusion should be explored, which will result in a decrease in binder content. The use of reinforcement and recycled aggregate can help to increase the sustainability of these mixes. While increasing the use of industrial by-products is a step toward sustainability, challenges with stability act as a barrier to their usage. In this context, novel valorization methods for utilizing waste feedstock into value-added products via the 3DP technique should be investigated. From a process standpoint, innovative print head designs may be capable of accommodating coarse aggregate more effectively.

5. Rheology properties

The rheological properties of GP are volume-and viscosity-dependent [182]. The processes of 3DP concrete require a wide variety of rheological characteristics than fresh concrete. Whilst pumping and extruding need a mix with low viscosity and yield strength, the concrete should have a high yield strength through production to minimize collapse or deformation due to the stresses of the subsequent layers [183]. This criterion implies that 3DP concrete should demonstrate a fast development of yield strength through time, allowing it to transfer swiftly from a pumpable mix to a high yield-strength mixture. It may be performed in two methods: by activating a tiny fraction of a big batch just before deposition [184] or by continually creating small batches with a high early-age strength [185]. Whilst the former technique accomplishes this by adding additives through the early blending process, the last method accomplishes this by intervening at the print head to increase constructability [185]. Both methodologies enable the mechanism of strength gain over time to be divided into 3 stages: (1) reflocculation, which begins within the first minutes following depositing; (2) setting owing to chemical reactions; (3) hardening owing to continuous curing and chemical reactions.

In 3D concrete printing processes, two competing modes of failure are distinguished: material failure by plastic yielding, and elastic buckling failure through local or global instability [186]. Elastic buckling, plastic collapse, or a combination of the two are all regarded as symptoms of fresh concrete's instability while installation, referring to low constructability in 3DP concrete. While the stiffness of concrete is responsible for the elastic buckling failure, the yield strength of fresh concrete is responsible for plastic collapsing [136,187–192]. Consequently, in addition to its yield-strength, the stiffness of concrete plays a significant role in

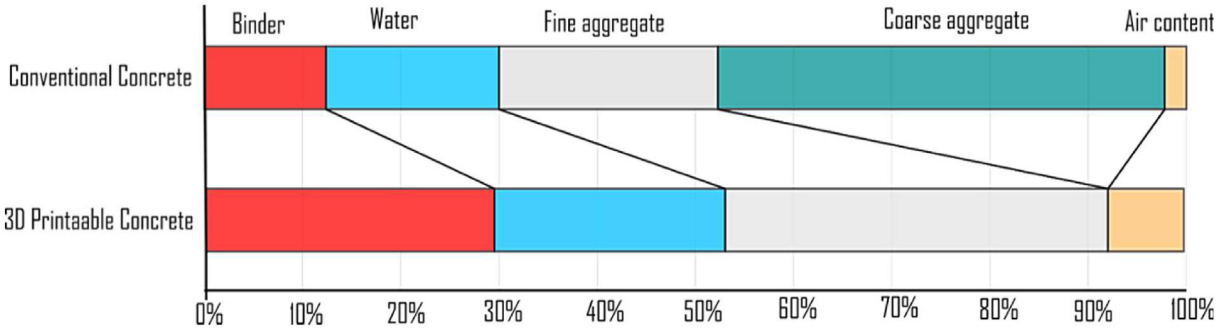

Fig. 17. An illustrative contrast of materials utilized in standard concrete and 3DP concrete [181].

influencing its constructability. Plastic collapse failure may be predicted by correlating the development of yield strength or the rate of construction with the increase of the concrete's strength with time [191]. The relationship between filament's shear stress and applied normal load from subsequent layers is very compatible with the Mohr-Coulomb failure criteria [136,139,186,191,193,194]. During printing, tri-axial stresses are applied to a part of the bottom layer, known as the crucial layer in 3DP concrete [191]. When the component in the bottom layer is exposed to vertical stress from subsequent layers, it deforms in the lateral, vertical, and longitudinal orientations [195]. Due to the constriction provided by the subsequent filament and the print platform, such deformation is minimized, leading to three-dimensional tensions. Although measuring stresses in every orientation experimentally is difficult, the requirement for a relationship between construction rate and strength increase complicates matters further.

In general, the rheological properties of concrete are impacted by the design mix, which comprises the volume percentage of the binding composites; aggregate properties, which include the size, shape, and distribution of particles; and the composition, which comprises the inclusion of GPs. Chemical additives have the potential to be a very efficient way of adjusting rheological behavior. Viscosity modifying compounds, which increase the viscosity of plastics, and superplasticizers, which act as dispersants to minimize yield-stress [145,189,196,197], are now commonly used to manage workability in concrete [198,199]. Thixotropy enhancers are also present in clays [200,201]. Optimizing rheology is crucial for successful additive manufacturing (AM). This is accomplished by the use of suitable admixtures, presumably in combination. Since physical processes alter their rheological properties, the majority of them are deemed chemically inactive. Nevertheless, as with superplasticizers that affect the rate of hydration of cement [202,203], they can have significant physical and chemical consequences. With such a diverse range of chemical additives, collateral impacts should be evaluated in addition to the admixture's main aspects [204].

The addition of thixotropic additives to 3DP concrete boosts its yield strength without affecting the rate of hydration of cement in the initial stages [157,205,206]. Owing to colloidal particle flocculation and continual nucleation, the thixotropy property of printed materials manifests itself in OPC-based GPs [154]. After the thixotropic material has been produced by optimal mix design, it may be adjusted by varying the admixture mixtures with the rate of a structural component [152]. Reiter, Wangler [155] investigated the effect of admixtures on the rheological characteristics of cement and the development of structures, emphasizing the need for building yield-stress to permit the vertical production of concrete prints. The average strength required to support a single layer is between 180 and 1000Pa, while the lower layer needs an average strength of 12 KPa to support a 1-m structure, as shown in Fig. 18.

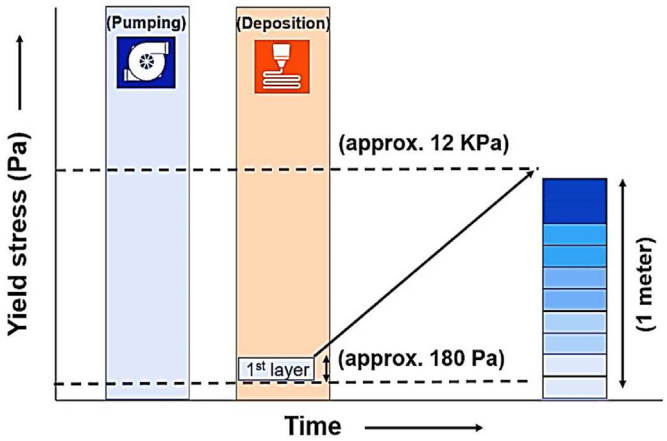

Fig. 18. A schematic representation of the evolution of the bottom layer yield strength with a building height [73].

Al-Qutaifi, Nazari [160] produced a fiber-reinforced GP mixture for the AM of concrete buildings. According to the authors, the inclusion of steel fibers resulted in bond dissociation issues, resulting in the failure of 8% of specimens. The addition of 0.5% polypropylene fibers reduces workability by approximately 33% due to the fiber's high absorbency of GP paste.

Panda, Unluer [73] developed a GP composite based on nanoclay and fly ash to improve the constructability characteristics. The activator viscosity was shown to be critical in determining the ultimate viscosity. Because the GP process is fundamentally different from the OPC hydration reaction, a control measure of raw -materials quantities is required for 3DP concrete [207]. Due to the fact that the GP material is derived entirely from industrial by-products, it is challenging to get consistent material characteristics for the aforementioned uses. To circumvent the limitations of liquid silicate, Nematollahi, Bong [208] developed a one-part GP composed of silicate powder. Panda, Singh [209] also employed silicate powder to create a 3DP-geopolymer and discovered that it had improved printability compared to liquid silicates.

Furthermore, several researchers have reported that geopolymers (GPs) derived from fly ash (FA) or metakaolin (MK) have a better plastic viscosity but a lower yield-stress and poor thixotropy when used as 3DP materials [176,210–213]. As a result, in order to meet structural criteria, we must strengthen the structure's rheological characteristics. The yield-stress is related to the particle-to-particle contact, referred to as flocculation, while viscosity is primarily influenced by the alkali-activator's viscosity [73]. Flocculation at resting and de-flocculation during flow behavior is critical in 3DP applications. The thixotropy characteristic may be investigated by concentrating on the flocculation process since the rate of

Fig. 19. Sol-gel transformation in the thixotropy phenomenon [66].

flocculation has a significant effect on the viscosity restoration [66], as shown in Fig. 19. Thus, the parameters affecting the flocculation and deflocculation capabilities of GP may be classified into four categories: spacing, size, the interaction of particles, and alkali-activator viscosity.

From the perspective of 3DP material's rheological characteristics, as a suspension system, as particle separation increases, the liquid film thickness surrounding the particle that prevents particle-to-particle contact increases, lowering plastic viscosity, yield-stress, and thixotropic properties [73]. However, the flocculation rate increases when fine particles and a large surface area are present [163]. Furthermore, addictive particles (such as carboxymethyl starch, nanographite platelets, and ground-granulated blast-furnace slag [GGBFS]) used to improve the properties are always polar particles that can encourage flocculation via attraction or the presence of Van Der Waals forces between the particles and the supersonic characteristic [214,215].

While the rapid setting of mixes is recommended to achieve a higher initial compressive strength and to avoid collapse, it is well documented that reducing the setting time value has a detrimental effect on interlayer adhesion. Roussel [154] observed that increasing the printing duration among layers and the level of thixotropy decreases interlayer bonding in 3DP concrete mixes. The level of thixotropy was found to be the cause of cold joints. As a result, it was recognized that optimizing the concrete rheology is important in light of the distinct rheological needs of 3DP concrete mixes before and after extruded. It was previously assumed that this characteristic is provided by temperature changes in polymer-based three-dimensional components [216].

By and large, materials with low viscosity and high yield stress are acceptable for use in 3DP concrete. Lee, Kim [217] demonstrated that the yield-stress range of 0.6–1.0 kPa is acceptable for the extrusion ability of the GP mixture and the geometric stability coefficient should be between 0.85 and 0.90 depending on the specification. Zhang, Wang [218] studied the yield-stress and structural build-up of 3DP-geopolymer mix activated with various Si/Na ratios of alkali. The Si/Na ratio of the alkali-activator has been discovered to have a considerable effect on the buildability and extrudability of 3DP-geopolymers mixes. As a basis for development, it was established that increasing the Si/Na ratio of the alkali-activator lowered the viscosity and yield stress of the GP mixes, as shown in Fig. 20. Moreover, it was discovered that decreasing the Si/Na ratio of the alkali-activator accelerates the structure formation of the mixes. Moreover, according to Nematollahi, Xia [132], when the SiO_2/Na_2O ratio of the alkali-activator sol is 3.22, the resulting GP exhibits acceptable workability.

Panda, Paul [163] observed that the proper incorporation of GGBFS into the GP design mix is critical for 3DP concrete

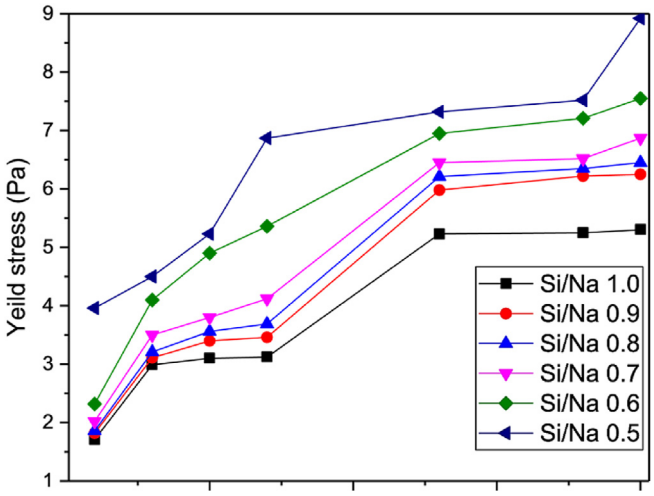

Fig. 20. The effects of the Si/Na ratio on the development of paste yield-stress [224].

performance. It was observed that, when the GGBFS concentration is increased from 5% to 15% by weight, the yield-stress increases with time, directly affecting workability throughout extrusion. Increased GGBFS content speeds the setting process (due to the rise in the rate of structural made), improving the constructability of 3DP concrete.

Panda, Singh [209] further investigated the development of GP yield-stress over time in order to gain a better understanding of structural creation and pump pressure throughout extruded. It was discovered that replacing 10% of FA with GGBFS (F90G10) greatly enhances yield-stress throughout the rest phase of 0 to 30-min, as shown in Fig. 21, which is attributable to the GGBFS particles accelerating the polycondensation process, resulting in early strength development. Another GP research discovered that substituting GGBFS for 40% of the FA led to a rise in the viscosity of 20%, yield-stress of 80%, which was ascribed to the faster reaction caused by the amorphous phases of GGBFS and interlocked impact. Increased yield-stress allowed for the construction of up to ten layers without deformation.

Zhong, Zhou [219] reported the development of porous GP composites via direct ink writing (DIW). A suitable ink with the appropriate rheological properties is critical to an effective DIW method [220], especially because such an ink must undergo the geopolymerization interaction, which constantly alters its rheological behavior at various stages (gelation/condensation/polymerization/hardening). Specified additives like graphene oxide (GO), Acti-Gel, and cellulose (AGC) [221] polyacrylic acid sodium

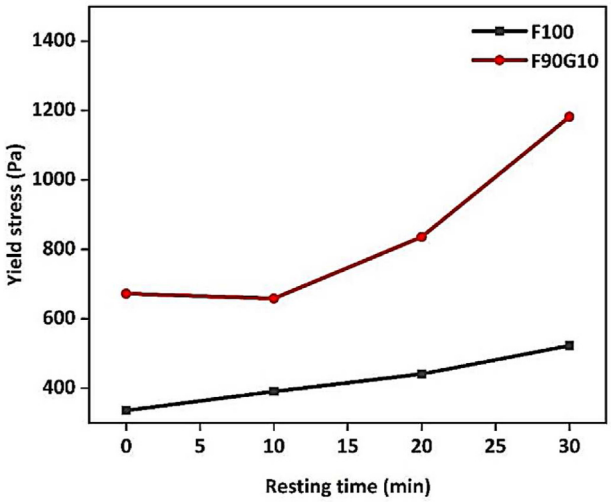

Fig. 21. Alteration in yield-stress of GP control mortar (F100) and mortar containing GGBFS (F90G10) with time [66].

salt (PAA) [220], and polyethylene glycol (PEG) [222,223] were introduced to the GP slurry to alter the dynamical rheological characteristics with time. Additionally, AGC, PAA, and PEG worked as rheological enhancers. Graphene has been regarded as a possible reinforcement or filler for ceramics [224], metals [225], polymers [226], and other materials [227]. Previously published work by Zhong, Zhou [219] showed that the addition of graphene oxide (GO) to a GP slurry improves the rheological properties, making it suitable for DIW as shown in Figs. 22 and 23. Moreover, Table 4 presents additional data on the effects of additives, minerals, alkaline activators, and reinforcement parameters on the rheological properties of 3DP-geopolymers.

6. Mechanical properties

6.1. Bond, compressive, tensile, and flexure strengths

3DP-geopolymer materials should have a strong bond between the layers and an early strength to minimize collapse and deformation induced by the top pressure. To meet the requirements of the actual structure, the brittleness and low flexural strength of GP should be enhanced [64]. As a result, several researchers conducted numerous experiments to improve mechanical characteristics, as summarized in Table 5.

The mechanical characteristics of 3DP-geopolymer materials may be modified in two ways: via building processes and using additive materials. The printing speed, printing time gap, and nozzle standoff distance are all aspects of the building process. The bond-strength of 3DP-geopolymer decreases with increasing time gap, owing to the fact that the interface layer's properties vary with

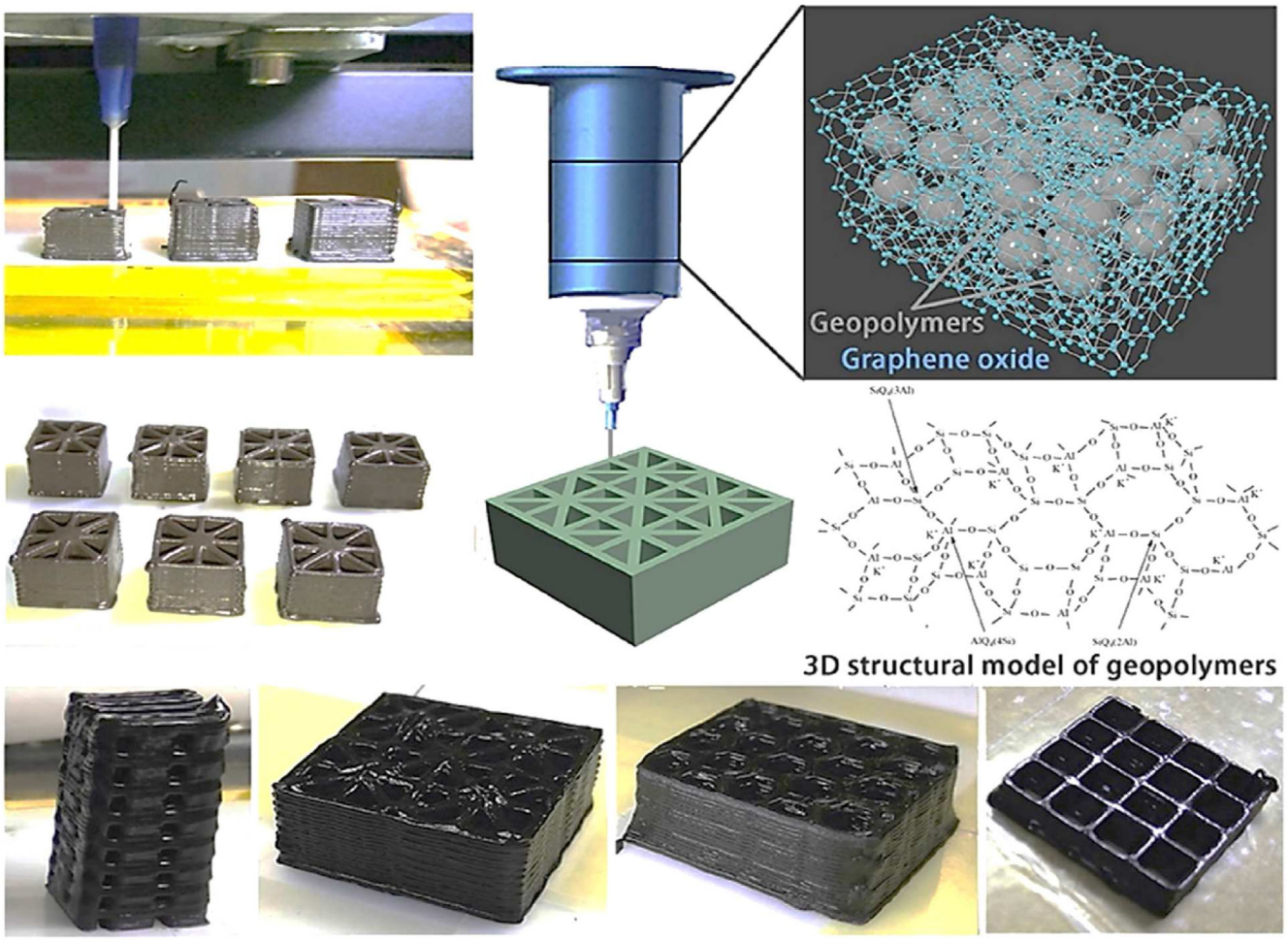

Fig. 22. The process and some structures of 3DP-geopolymers. Besides, the chemical composition of geopolymers. It is worth noting that the colors of the printed samples change from brown to black when the graphene oxide (OG) loading is increased [219].

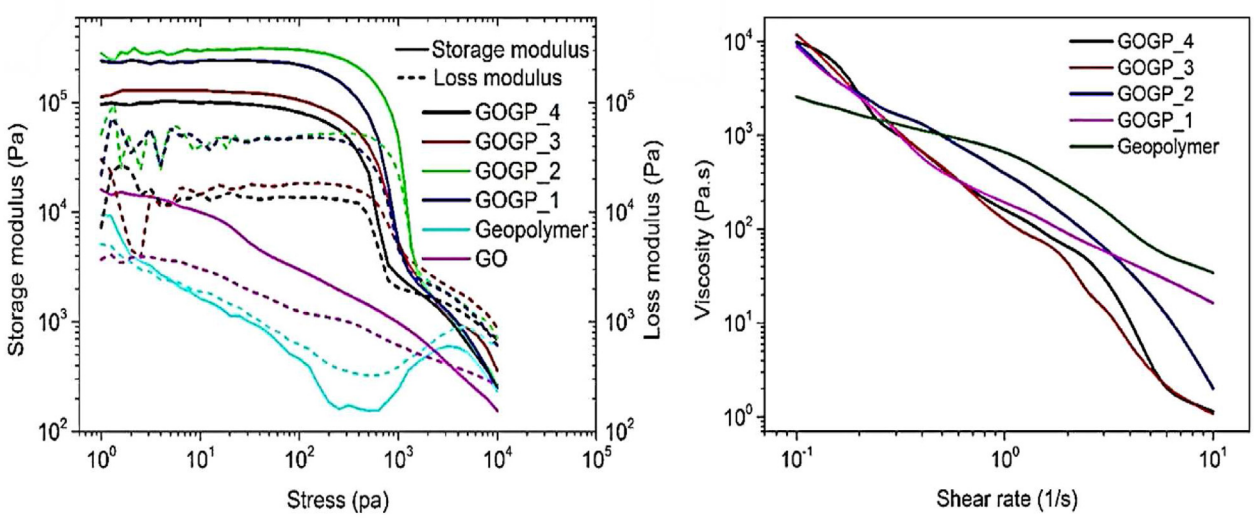

Fig. 23. Rheological behavior of the GO/geopolymer ink [219].

Table 4
Effects of additives, minerals, activators, and reinforcement parameters on the rheological characteristics of 3DP-geopolymers.

Parameters	Type	Scope	Noticeable results	Optimum value	Refs.
Additives and minerals	Water/binder ratio	0.30–0.35	Yield-stress = 0.414–1.161 kPa; Plastic viscosity = 7.41–12.71 Pa	0.30	[228]
	Borax (wt%)	4–9	Yield-stress = 16–20 Pa Yield-stress = 0.2 kPa	4	[229]
	Solid/binder ratio	1.10–1.9	Yield-stress = 0.39–0.8–1.63 kPa	1.50	[65]
	Coarse aggregate (wt%)	40–60	Yield-stress = 0.0135–0.0186 kPa	40	[214]
	Fine aggregate (wt%)	40–60	Plastic viscosity = 6.83–11.04 Pa s	60	
	Fly ash (wt%)	90–100	Yield-stress = 0.34–0.68 kPa Thixotropic index = 0.25–0.36	90	[66]
	Silica fume (wt%)	0–10	Viscosity recovery = 0.26–3 kPa s	10	
	GGBFS (wt%)	0–10		0	
	Clay (wt%)	0–0.50	Yield-stress = 1.42–7.71 kPa; Apparent viscosity = 17.62–18.83 Pa s	0.50	[73]
	Water/solid ratio	0.3–0.35	Yield-stress = 4.42–7.71 kPa; Apparent viscosity = 15.4–18.83 Pa s	0.30	
	Hexaboron nitride (wt%)	0–4.0	Apparent viscosity = 4950–30,000 Pa s Shear modulus = 4850 kPa	4	[230]
	Urea (%)	0–5.0	Yield-stress = 2.61–43 Pa; Plastic viscosity = 20,000–200,000 Pa s	3	[231]
Alkaline activator	Si/Na	0.5–1.0	Yield-stress = 0.34–3.44Pa	0.50	[218]
	Na_2SiO_3 (wt%)	6.4–22.2	Yield-stress = 0.52–0.60 kPa	6.40	[232]
	NaOH (wt%)	22.2–31.9		31.90	
	Activator (wt%)	10–20	Yield-stress = 3.36–4.21 kPa Apparent viscosity = 7.3–8.07 Pa s	20	[209]
	H_2O/Na_2O	22.38–42.20	Yield-stress = 0.06–1.71 kPa	22.39	[206]
	SiO_2/Al_2O_3	4.20–4.41	Apparent viscosity = 210–1000 Pa s Plastic viscosity = 30,000–100,000 Pa s	4.41	
Reinforcement	Micro crystalline cellulose	0–1.50	Yield-stress = 0.412–1.21 kPa; Plastic viscosity = 7.42–8.95Pa	1	[228]
	Nano graphite platelets	0–1.0	Yield-stress = 11.96–36.42Pa; Plastic viscosity = 6.62–17.26 Pa s	1	[214]
	Wollastonite	0–0.065	Yield-stress = 1–2.50 kPa	0.065	[233]
	Attapulgite nano - clay (wt%)	0–1	Yield-stress = 1.21–1.7 kPa	1	[234]
	Plastic viscosity fibers (wt%)	0–0.5	Yield-stress = 1.21–1.36 kPa	0.25	
	Wollastonite (g)	2–21	Apparent viscosity = 149–800 - more than 6000 Pa s	10	[235]

time, and the shorter the time gap, the tougher the layer is and so has a higher bond strength [163]. The bonding strength decreases somewhat as printing speed increases, and the nozzle standoff distance affects the precision of the bead deposition pattern [72,133,236], for example, Panda, Paul [163] show that the nozzle distance equivalent to the layer height is best for print quality and bond strength. Increasing the distance causes filament deformation. The standing distance between the nozzle and the printing platform is the distance between the nozzle and the printing substrate.

Bond strength and interlayer weak interaction are thought to be critical issues in 3DP production [43,158,237–243]. Bond strength denotes the condition of surrounding materials, which is mostly controlled by the rate of material strength growth and 3DP parameters. Because the entire item is constructed layer-by-layer in the GP, adequate bond strength is required to assure the structure's reliability and stability [132]. The occurrence of cold joints and the weak interactions across layers are proportional to the printing materials' properties and layering intervals duration [2,97,244–246]. Although the bonding strength between successive layers diminishes with increasing time of resting, the structural build-up factor rises as a result of succeeding layer shape preservation [247]. Therefore, Roussel [154] suggested a critical resting time to reduce layer interface flaws. Muthukrishnan, Ramakrishnan

Table 5
Impacts of minerals, admixtures, activator, and printing factors on mechanical characteristics of 3DP-geopolymers.

Parameter	Type	Scope	Mechanical Results (MPa)	Optimum values	Refs.
Minerals and admixtures	Water/binder ratio	0.30–0.35	Com. Str. = 49.5–59 Flex. Str. = 11.7–13	0.3	[228]
	Silica fume (wt%)	0–10	Com. Str. = 5.3–8.5	0	[229]
	Fly ash (wt%)	0–60		0	
	Borax (wt%)	100–800		100	
	Magnesia (wt%)	40–100		100	
	Powder systems	Plaster - based powder GGBS + Na_2SiO_3 + Sand	Com. Str. = 0.69–0.91	GGBS + Na_2SiO_3 + Sand	[48]
	GGBS (wt%)	0–100	Com. Str. = 24.9–29.6	100	[133]
	Fly ash (wt%)	0–100		0	
	Binder saturation (%)	70–170	Com. Str. = 12.9–19.3	170	[250]
	Aggregate (wt%)	60–120	Com. Str. = 43–53.2	72	[135]
	Copper tailing (wt%)	0–60		48	
	Water/binder ratio	0.22–0.24	Ten. Str. = 5.32–5.66	0.22	[265]
	Solid/binder ratio	0.20–1.20		0.2	
	Sand	Concrete, Gneiss, Brick	Com. Str. = 1.36–5.60 Flex. Str. = 1.26–2.35	Gneiss	[266]
	Sand type	Quarry waste	Com. Str. = 11.6–12	Silica sand	[267]
	Binder quantity (μl/mm)	Silica sand 0.5–1	Com. Str. = 11 - 12	0.5	
	Nanoclay (wt%)	0–0.5	Com. Str. = 24 - 32	0	[73]
	Admixture type	Without admixture Urea Naphthalene Polycarboxylate	Com. Str. = 15.6–32	without admixture	[268]
	Aggregate type	Limestone sand Seashell sand Glass sand	Com. Str. = 33 - 50 Flex. Str. = 6.1–7.7 YM = 2000 - 2900	Glass sand Limestone sand	[269]
Activator	MR	1.6–2.0	Ten. Str. = 0.339–0.735	2	[270]
	Activator and composition	NaOH(1.50–3) + N Grade Na_2SiO_3 NaOH (1.50–3) + D Grade Na_2SiO_3 KOH (1.50–3) + KASIL 2236 Grade K_2SiO_3 KOH (1.50–3) + KASIL 2040 Grade K_2SiO_3	Com. Str. = 8.6–16.7	D Grade Na_2SiO_3 + NaOH SS/HS = 3.0	[271]
	Si/Na	0.5–1.0	Com. Str. = 37.91–53.05	0.9	[218]
	Activator and composition	NaOH (1.50–3) + D Grade Na_2SiO_3 (1.50–3) + KASIL 2040 Grade K_2SiO_3 + KOH NaOH (1.50–3) + N Grade Na_2SiO_3	Com. Str. = 8.6–16.7	D Grade Na_2SiO_3 + NaOH (SS/HS = 3.0)	[272]
	Activator and composition (wt %)	Anhydrous Na_2SiO_3 (0–0.10) GD Grade Na_2SiO_3 (0–0.10)	Com. Str. = 34–56.8	GD Grade Na_2SiO_3 (0.1)	[176]
	Activator contents (%)	10–20	Com. Str. = 19–43.8	20	[209]
Printing	Time gap (min)	5–15	Flex. Str. = 3.36–5.5	5	[160]
	Layer dimensions (mm)	160 × 13.33 × 40 and 160 × 40 × 13.33	Ten. Str. = 0.30–1.44	160 × 40 × 13.33	[221]
	Time gap (min)	0–20		0	
	Time gap (min)	2–15	Com. Str. = 33.5–35 Flex. Str. = 5.3–6.1	2	[132]
	Printing orientation	Inclined Rectangular Orthogonal	Flex. Str. = 9.95–28.8	Inclined	[10]
	Time gap (min)	2–15	Com. Str. = 39.6–43.2 Flex. Str. = 5.4–6.2 IBS = 1.6–2.0	2	[132]
	Printing layers	1–2	Com. Str. = 34.6–39.0 Flex. Str. = 8.7–10.2	2	[273]
	Filament-heating(s)	0–20 0–10	IBSs = 0.45–1.24 YM = 289.63–2048	10	[9]
	Time gap (min)	1–20	Ten. Str. = 0.4–1.45	1	[163]
	Nozzle-height (mm)	0–4	Ten. Str. = 1.53–2.4	0	
	Printing speed (mm/s)	70–110	Ten. Str. = 1.6–1.69	70	
	Printing speed (× 10 - 6 m/s)	62–248	Flex. Str. = 15	62	[274]
	Binder rate (mg/s)	100–180	MORs = 2.4–4.5	135	[275]
	Printing orientation	Inclined Rectangular Orthogonal	Com. Str. = 25.7–41.7 Ten. Str. = 1.67–4.69 Shear strength = 6 - 12	Rectangular Orthogonal	[276]

[9] used a rapid microwave heating process to repair the weak interlayer connections in GP composites.

Moreover, Panda, Paul [163] investigated the tensile bond strength of printed GP mixtures. The FA utilized was classified as class F in accordance with American Sociey for Testing and Materials (ASTM) C618-12a. Following 20-min, substantial growth in viscosity and yield-stress of the material is noted, making extrusion virtually impossible. The density of printed samples was reported to be around 5% greater than that of casted samples, which is presumably owing to the high pressure used through the extrusion process. Several similar investigations were addressed before having demonstrated an increase in the strength of printed samples when loaded in a specific direction [153]. Analyzing the effect of printing time gaps of 5-, 10-, 15-, and 20-mins revealed that as the printing time gap grows, the tensile bond strength declines, as shown in Fig. 24. The sticky property of the potassium silicate [K_2SiO_3] aids in bonding during the initial few mins. As the printing time gap widens, polycondensation in GP stiffens it, reducing bonding strength. Following 20-mins, printing became problematic, and a new batch was placed, and printed samples were analyzed for bond strength at time intervals of 35-, 180-, and 360-mins. It was discovered that the tensile strength at a 35-min time interval was increased owing to the freshness of the new batch. Nevertheless, when the time gap increases, the tensile strength decreases owing to a moisture transfer phenomenon produced by the surface's dryness trapping air voids.

On the other hand, due to the anisotropic nature of the printing process, the mechanical characteristics and linear dimensions of 3DP-geopolymers strongly depend on the loading direction [221,248]. For example, Paul, Tay [153] investigated the effect of printing orientation on the concrete mixture. For mixes without fibers, 8 mm diameter circular nozzles were used, and for mixes containing glass fibers, 10 × 20 mm rectangular nozzles were used. The orientation of printing has a significant effect on the strength of the 3DP specimens. When compared to casted samples, a good printing orientation can increase strength by up to 15%. Circular nozzles produce more voids than rectangular nozzles and are also more adapted to complicated designs.

According to Nematollahi, Xia [132], when the SiO_2/Na_2O ratio of the alkali-activator sol is 3.22, the resulting GP exhibits acceptable strength and expansibility, and a good capacity for shape retention. Furthermore, Panda, Unluer [73] found that adding 1% clay has a beneficial effect when the water/solid ratio is 0.30 and the activator/binder ratio is 0.35. In another study by Panda, Ruan [207], including 2% of water graphite seedlings in a hybrid system of alkali-activated slag and 0.4% nanoclay, hydration is improved, and the structural accumulating rate demanded large-scale 3DP is increased. Also, the compressive strength of 3DP-geopolymer concrete made with 50% FA and 50% GGBFS is 25 MPa, which is sufficient for a wide range of sectors [133]. Besides, as shown in Fig. 25, by directly and automatically adding 1.2 mm continuous micro-wire ropes into GP composites after the filaments of 12 mm were deposited, the mechanical strength, toughness, and deformation of GP composites subsequent to cracking were greatly enhanced [10,249].

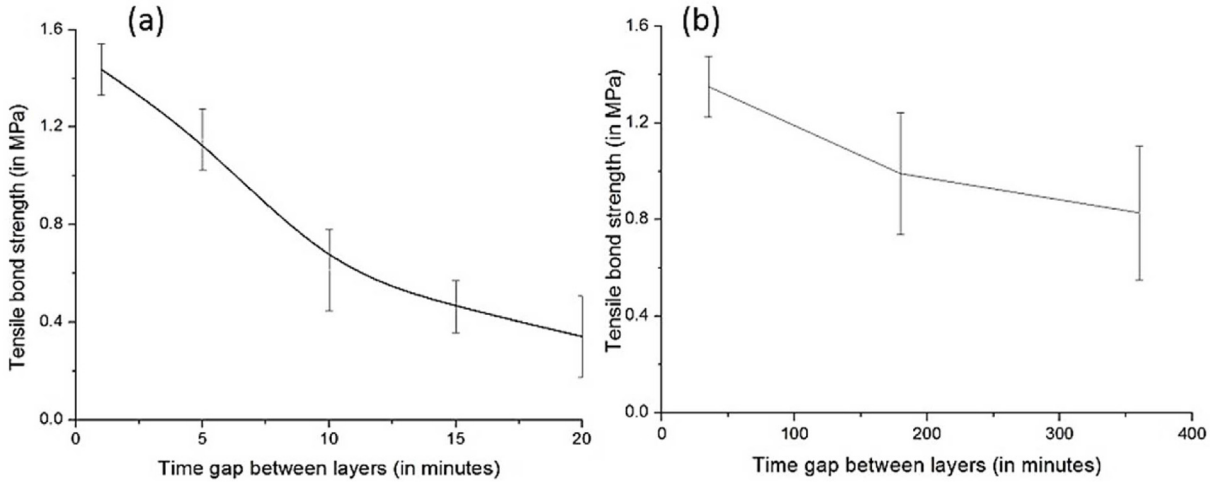

(i) Influence of time gap for (a) same (b) different mix materials.

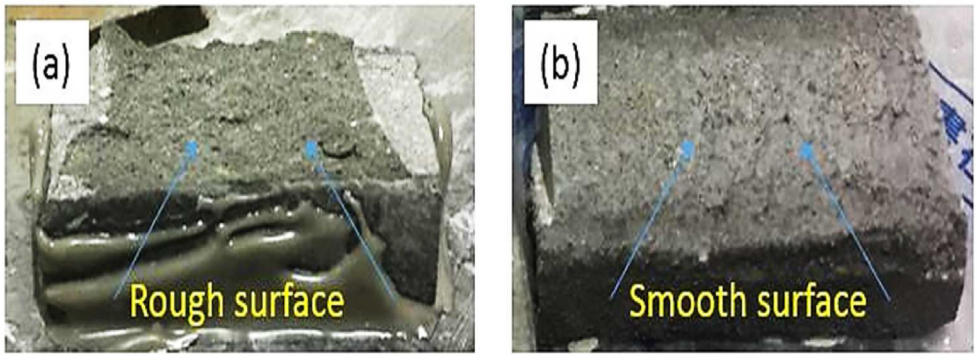

(ii) Bond test failure patterns for (a) one-minute time gap (b) the fifteen-minute time gap

Fig. 24. Influence of printing time gap between layers on the tensile bond strength [163].

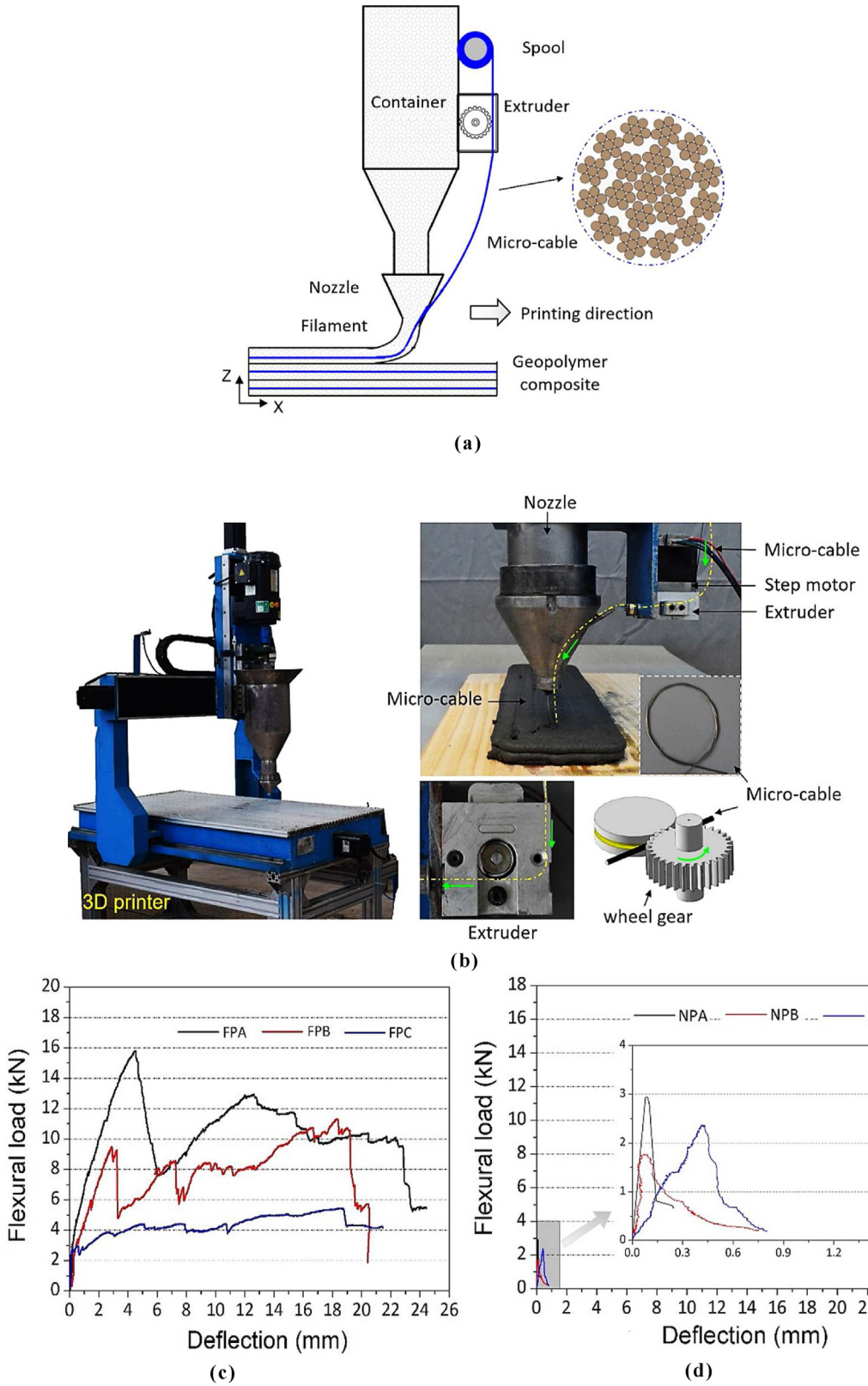

Fig. 25. (a) Schematic illustration and (b) Set-up of 3D printer and entertaining process of micro-cable into geopolymer filaments; (c) flexural characteristics of printed GP with and (d) without reinforcement [10].

Xia, Nematollahi [133], Xia, Nematollahi [250] demonstrated the feasibility of using GPs as a binder jet 3DP material. A powder blend of FA, GGBFS, and sodium silicate was blended with an alkaline sol to achieve a compressive strength of 25 MPa. As a consequence, all printing samples are limited to dimensions of 20 × 20 × 20 mm. Nonetheless, an earlier study conducted by the same researcher discovered that the effect of processing subsequently on compressive strength decreased as the size of the printed specimen

rose as shown in Fig. 26. This finding was assigned to the sample since the alkaline sol was unable to penetrate it. Consequently, it is critical to creating a clear relation between the depth of penetration of the storage solution subsequent to processing and the resultant composite's compressive strength increase. An additional technique must be established to improve the penetration of the storage solution subsequent to processing. Apart from that, it is critical to study if two distinct types of alkali-activators can be used to raise the required strength.

On the other hand, the function of addicting materials is primarily to alter the chemical reaction, porosity, and bridge the fractures of 3DP-geopolymer materials. Previously published work by Zhong, Zhou [219] showed that adding graphene oxide to a GP slurry not only altered its rheological characteristics, making it acceptable for direct ink writing but also served as a contributing reinforcement phase, enhancing mechanical strength and electrical characteristics. Moreover, the compressive strength and flexural strength both declined significantly as carboxymethyl starch addition increased. The increased concentration of water-soluble carboxymethyl starch decreased the interfacial tension of the paste's aqueous phase, allowing for more air to be admitted into the paste and increasing its porosity [215]. With the inclusion of GGBFS, GGBFS can dissolve in the alkaline regent and provide additional heat, hence speeding up the polycondensation interaction and increasing the early compressive strength.

On the other hand, a glass fiber-reinforced matrix including clay led to more printable GP mixes [65,251]. Anisotropy, which is a recognized intrinsic difficulty of AM [252], is another hurdle that GP-based materials must overcome because of their non-uniform mechanical characteristics in various orientations [253,254]. fiber

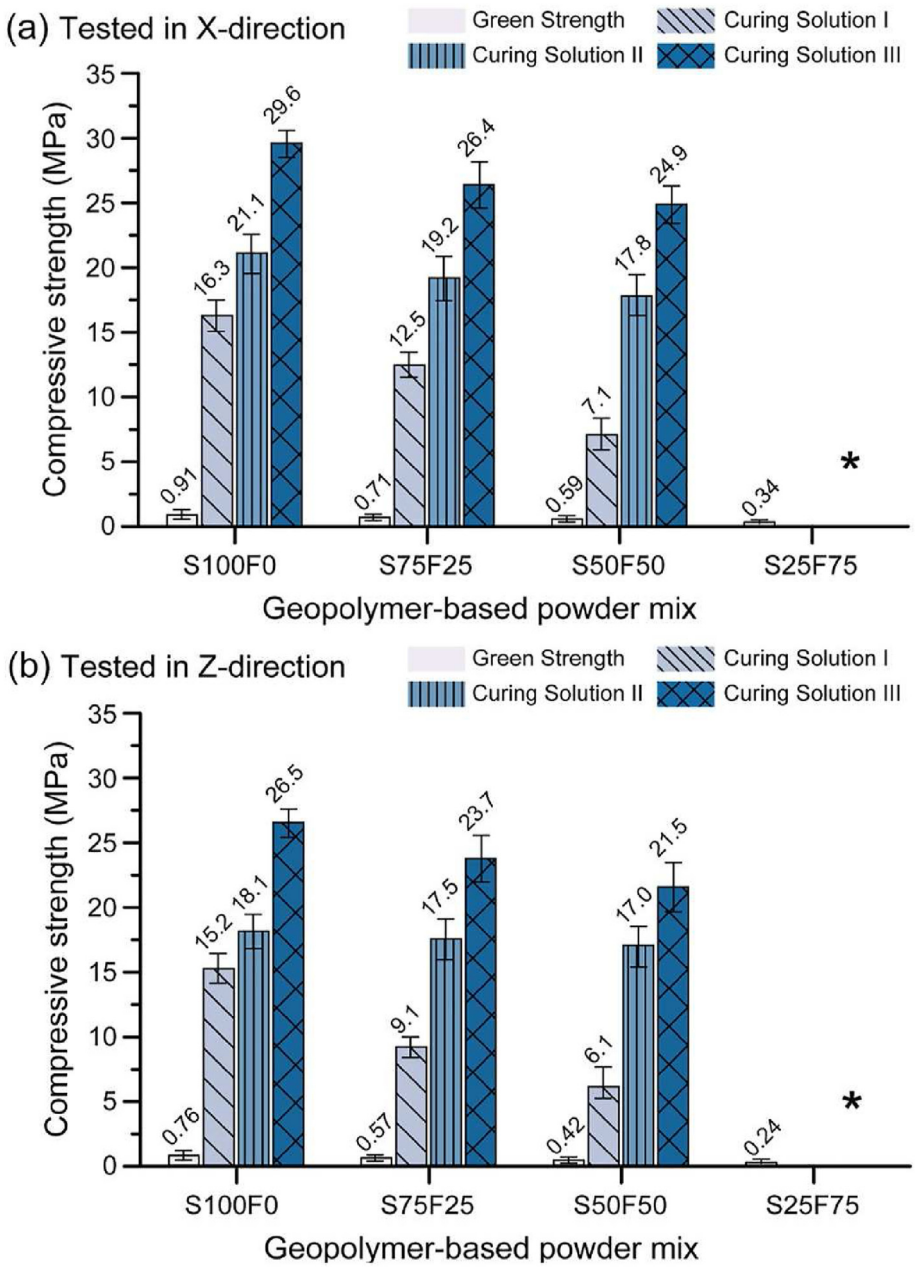

Fig. 26. Compressive strength of green and 3DP cubes following processing after 7 days, evaluated in (a) X-Direction and (b) Z-Direction [133].

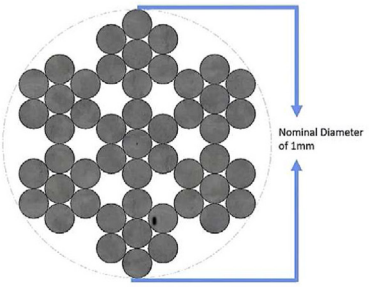

(a)

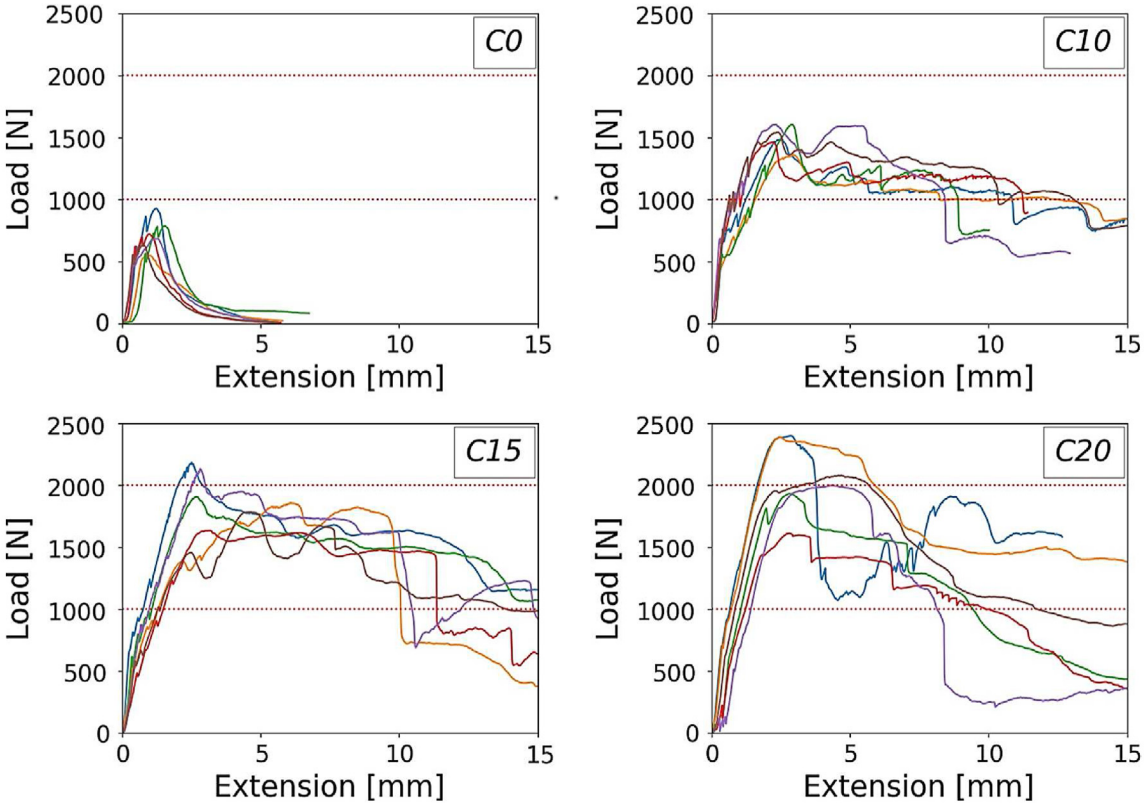

(b) Load versus displacement graph for reference (C0) and C10, C15, C20 geopolymer composite, where C10, C15, and C20 represent matrix reinforced with stainless steel cable of 1, 1.5, and 2mm, respectively.

Fig. 27. (a) Cross-section of stainless steel cable, and (b) load vs displacement graphs (helps to describe flexural properties of the GP composite) of the reference group and three sets of samples [64].

reinforcement can improve the structural stability of 3DP materials to a certain extent due to the matrix's higher tensile strength and flexural strength capabilities [239,255–258]. Lim, Panda [64] addressed the structural stability issue in GP-based materials by combining a cable extruder with a nozzle output as shown in Fig. 27. According to the authors, the inclusion of fibers can enhance flexural strength by bridging cracks [64,163,247].

Al-Qutaifi, Nazari [160] produced a fiber-reinforced GP mixture for AM of concrete buildings. The goal of the fiber reinforcement was to strengthen the interface bond among adjacent layers. The GP mixture contains 200 gm sand and FA, as well as an activator/binder ratio of 0.26. To increase the hardened characteristics of this mixture, polypropylene and steel fibers were added. For samples with layer dimensions of 160 × 40 × 13.3 mm, maximum flexural strength of 5.46 MPa was obtained. In an additive process, which was carried out during this case with the use of specific timber molds, it is found that the addition of 1% steel fibers raises flexural strength by 20%, compared to an almost 100% rise in tensile strength in traditional concrete. Additionally, it was discovered that the addition of steel fibers resulted in bond separation problems, resulting in the failure of 8% of specimens.

Because the placement of steel bars is incompatible with 3DP technology, its progress is stymied to some extent. Strain-hardening cement-based composites, being one of the most effective ductile materials in structural engineering, offer enormous potential for usage in 3DP [259–263]. Li, Bos [256]investigated the

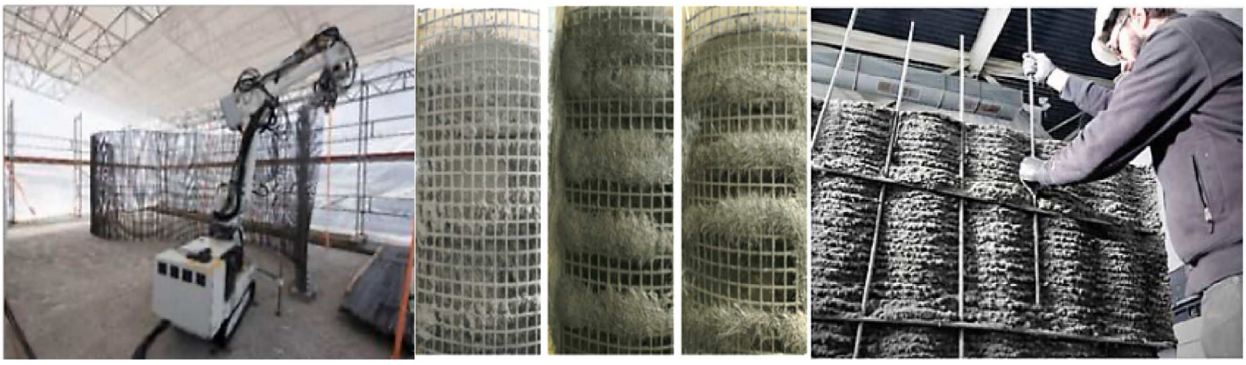

Printing after placing reinforcement [285].

Installation of reinforcement mesh before printing [285].

Placement of reinforcement after printing [286].

The structure printed with reinforcement before printing [62].

Fig. 28. Examples of 3D-printed concrete reinforcement methods.[285], [285], [286], [61].

use of strain-hardening cement-based composites in 3DP and showed that the presence of an interlayer interface does not affect the multiple cracks and strain hardening of 3DP strain-hardening cementitious composite materials under tensile stress. Yu, McGee [264] further validated the equivalent performance of 3D-strain-hardening cement-based composites and standard strain-hardening cement-based materials by printing a 1.5-m-tall twisting column with 150 layers. This research lays the groundwork for the effective fabrication of 3D-strain-hardening GP composites by combining 3DP with strain-hardening composite materials. Moreover, Table 5 presents additional data on the influences of minerals, admixtures, activator, and printing factors on mechanical properties of 3DP-geopolymers.

6.2. Reinforced 3DP-geopolymer concrete

It is well recognized that the most often used way of increasing the ductility or tensile strength of traditional concrete is to incorporate steel reinforcing [277–279]. It was highlighted that it is extremely hard to add steel reinforcement automatically and directly to 3DP concrete mixes in aim to discuss these unfavorable characteristics. To gain acceptance of 3DP concrete as a viable substitute for traditional concrete, however, it is important to enhance the ductile behavior of the printed samples and minimize fracturing and deformation. As a result, it was recognized that overcoming this obstacle is important [280,281]. To this aim, it was discovered that several different ways of reinforcing 3DP concrete combinations had been offered. A rebar cage is physically inserted prior to printing in the approach provided by the Chinese construction company Hua Shang Tengda, and then concrete mixes are printed in layers using a double spraying technique. Fig. 28 illustrates the structure printed using this approach.

Moreover, it was noted that this technique is not commonly employed and that the mechanical properties of structures reinforced using this approach have not been evaluated [282]. By and large, it was concluded from the literature research that fiber reinforcement is preferable for strengthening [252]. According to their volume, stiffness, and length, the fibers are introduced into the mix throughout extrusion or mixing. Generally, it was assumed that flexible, short fibers are incorporated directly into the mix due to their ease of passage via the nozzle [255]. It was specified that hard and long fibers should not be added immediately to the mixture since they might harm and block the nozzle [283]. Kazemian, Yuan [142] observed that adding fiber with a length of 6 mm enhanced the compressive strength of 3DP concrete mixes but had no significant influence on the shaped stability index. Jo, Jo [62] conducted another investigation in which they studied the usage of polyvinyl alcohol fiber in 3DP concrete mixes to reduce shrinkage cracking. The researchers note that the optimum fiber proportion is 0.1% of the weight of cement. When fiber is used in excess of this

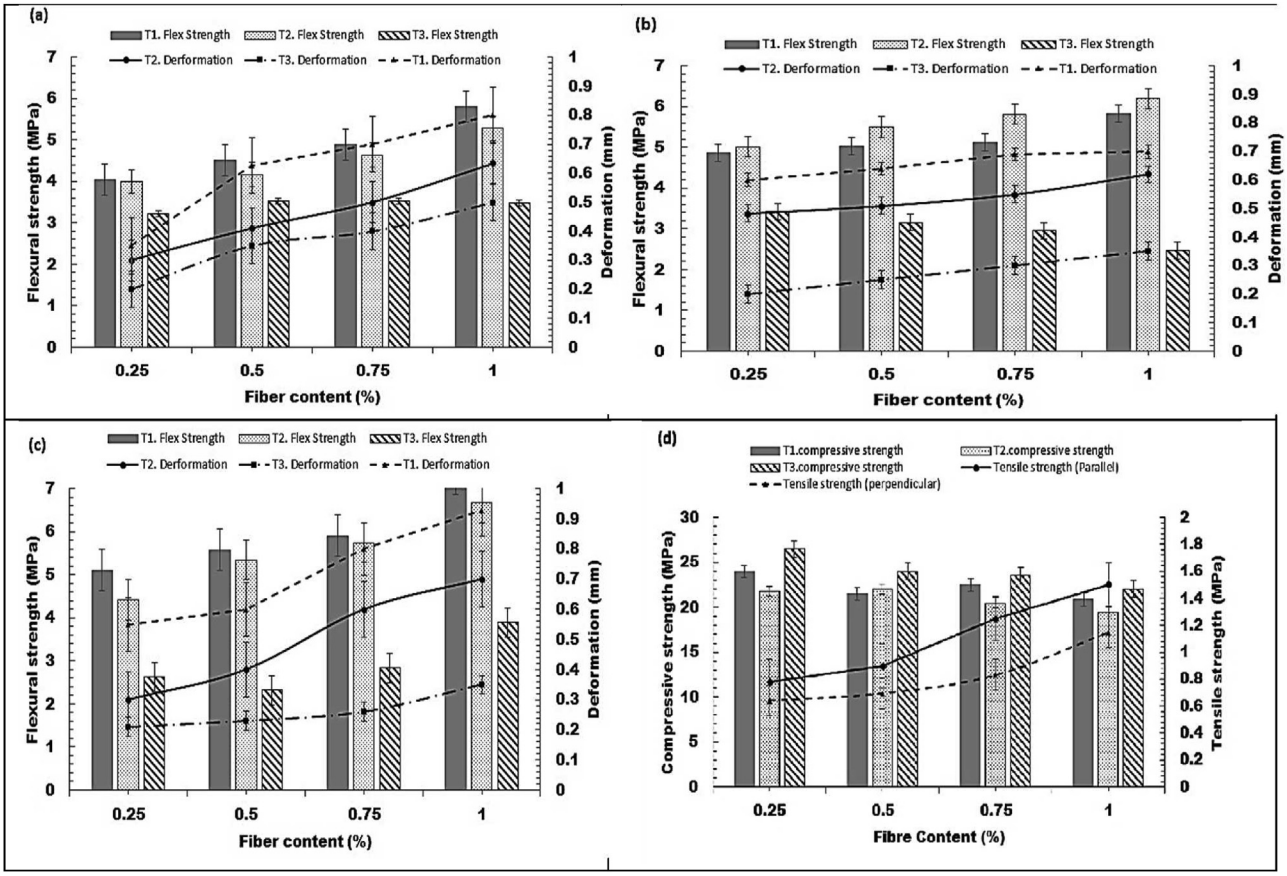

Fig. 29. Flexural characteristics of glass fiber-GP composite with (a) 3 mm (b) 6 mm (c) 8 mm fiber length and (d) compression/tensile properties with 3 mm glass fiber [251].

Table 6
Effects of reinforcement parameter on the mechanical properties of 3DP-geopolymers.

Parameter	Type	Scope	Mechanical Results (MPa)	Optimum values	Ref.
Reinforcements	Glass fiber (wt%)	0.25–1	Com. Str. = 22–26.5	0.25	[251]
	Glass fiber length (mm)	3–8	Flex. Str. = 5.8–7	8	
			Flex. Str. = 5.1–7	1	
			Ten. Str. = 0.8–1.5		
	Micro crystalline cellulose (wt%)	0–1.50	Com. Str. = 49.7–58 Flex. Str. = 11.8–12.4	1	[228]
	Reinforcement types	Without reinforcing Polyvinyl alcohol (PVA) para-phenylene benzobisoxazole (PBO) Polypropylene (PP)	Flex. Str. = 7.8–10.3 = 4 IBSs = 2.34–3.04	PBO fibers Without reinforcing	[284]
	Reinforcement types	Without reinforcement Carbon fibers Flax fibers	Com. Str. = 38.6–48.6 Flex. Str. = 6.95–9.45	Flax fibers	[287]
	Reinforcement types & wire diameter (mm)	without wire Steel wire (ø 1–2 mm)	Flexural load = 0.75–2.15 kN	Steel wire ø2 mm	[64]
	Reinforcement types	Without reinforcement PP-fibers (0–0.5%) Steel fibers (0–1%)	Flex. Str. = 5–6.3	Steel fibers (1%)	[160]
	Basalt fiber (wt %)	0–0.7	Flex. Str. = 2.36–4.56	0.7	[134]
	PP fiber (vol%)	0–1.0	Com. Str. = 18.3–35.8 Flex. Str. = 6.6–8.2	0.25 0.5	[288]
	Reinforcement types	with and without wollastonite micro fiber	Com. Str. = 48.4–49.2 Flex. Str. = 9.4–12	Without wollastonite micro - fiber With wollastonite micro - fiber	[233]
	Reinforcement types	with and without steel cable	Flex. Str. = 5.9–28.9	with steel cable	[10]
	high density polyethylene (HDPE) fibers (vol%)	0.30–1.50	Ten. Str. = 5.34–5.67	1.5	[265]

value, the nozzle becomes blocked. As shown in Fig. 29, Panda, Paul [251] studied the impact of introducing short glass fiber to the GP in large-scale 3DP concrete.

Lim, Panda [64] studied the influence of steel cable diameter on 3D printing geopolymer flexural strength. It has been demonstrated that increasing the diameter of steel cable can result in a

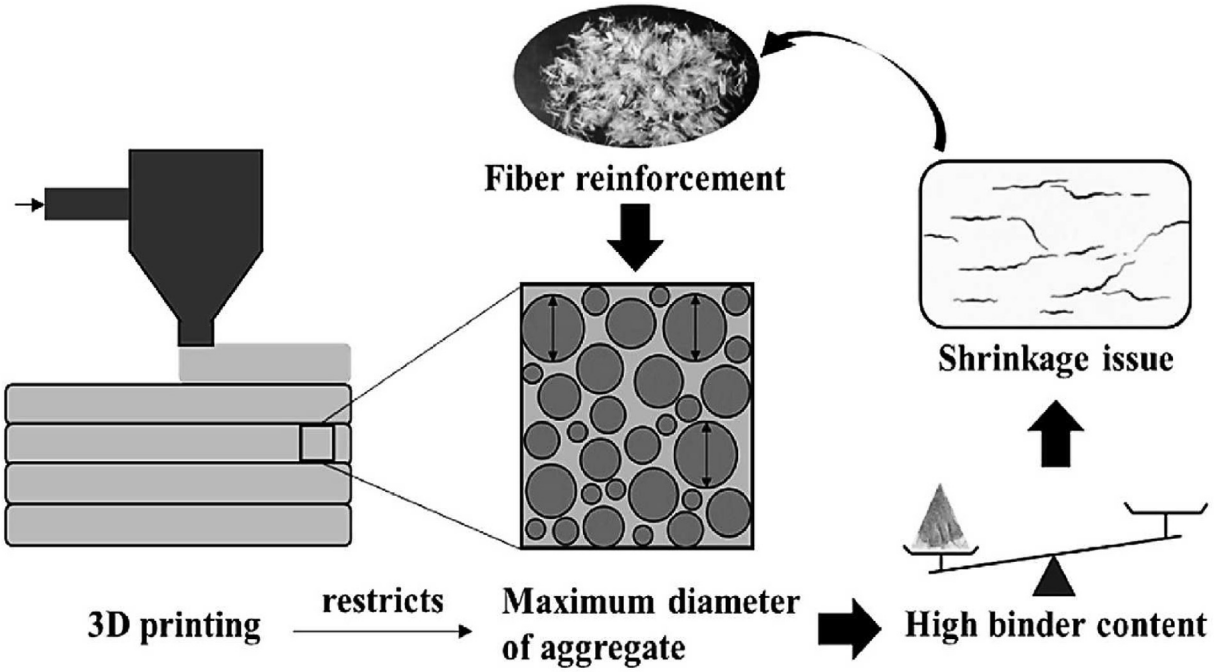

Fig. 30. The limitation to the parameters in mix design for 3DP technology [77].

continually increasing pattern in 3D printing geopolymer flexural strength. Ma, Li [10] showed similar significant benefits of employing steel cables while investigating the impact of printing paths and steel cable reinforcement on the flexural strength of 3D printing geopolymer. The researchers noted that reinforcing 3D printing geopolymer with steel cables increased flexural strength when compared to plain 3D printing geopolymer. Because of the improved fiber bridging behavior, Al-Qutaifi, Nazari [160] shown that geopolymer mixes containing 1% steel fiber outperform mixes reinforced with 0.50% PP fiber, independent of loading direction.

Bong, Nematollahi [273] found that PVA fibers, length 8 mm, have a positive effect on compressive strength. The compressive strength of the reinforced fibers ranges between 25 and 49.8 MPa, based on the printed layers and testing orientation.

Nematollahi, Xia [284] conducted research on FA-based geopolymers including three types of plastic fibers (each addition 0.25 vol% and 6 mm length): polypropylene, polyvinyl alcohol, and polyphenylene benzobisoxazole (Zylon®), the world's strongest fiber. The major purpose of adding fibers was to reduce the interlayer bond strength of 3D printed geopolymer. Extruding material from a nozzle was used to create the specimens. Following preparation, specimens were cured in an oven for 24 h at 60°C. The results reveal that the 3D printed fiber-reinforced geopolymer outperforms the ordinary specimens in terms of characteristics. Flexural strength ranged from 9 to 10.3 MPa and inter-layer bond strength ranged from 2.3 to 2.5 MPa based on the type of fiber; for ordinary specimens, these values were 7.7 and 3 MPa, respectively.

In summary, it was discovered that adding fibers enhanced compressive strength marginally but dramatically boosted tensile and flexural strength at a 1% amount. The fibers used in various 3DP concrete mixes are listed in Table 6. As illustrated in Table 6, various fibers ranging in length from three to eight can be employed in 3DP concrete blends. Additionally, it is assumed that the fiber percentage of the cement is between 0.2 and 1.0%. Moreover, Table 6 presents additional data on the effects of reinforcement parameters on the mechanical properties of 3DP-geopolymers.

7. Future challenges

The building industries that utilize 3DP technology are still in their infancy, and several obstacles must be addressed before this technique can be fully implemented. One of the most significant obstacles is the current scarcity of printed concrete. Overall, while numerous investigations on 3DP production have been conducted, there is a lack of appropriate design guidelines and standard test techniques, as investigators have highlighted [61,75,77,97,153,289–291]. Moreover, Mechtcherine, van Tittelboom [292] studied the specifics in characterizing the properties of additively manufactured, cement-based materials in their hardening and hardened states. According to the authors, the related challenges are associated with the printed material's layered structure, which results in higher degrees of anisotropy and inhomogeneity in comparison to conventionally cast concrete. Thus, in the production of test specimens, the particularities of the real-scale 3D-printing process must be considered. Therefore, concentrated research efforts are required to address the shortcomings of AM and 3DP buildings in the coming days, including buildability, rheology, interlayer bond, and structural integrity. Geopolymer materials provide significant potential for this new and creative construction sector due to their rapid strength growth at ambient and high temperatures [293–295], as well as their economic and environmental benefits [100,296]. According to the reviewed literature, investigators have achieved significant advancement and progress in fulfilling the rheological criteria of geopolymers. Even so, structure details, printing properties (layering intervals, printing speed, nozzle, and extruder details, etc.), and inherent problems (buildability, interlayer bonding, structural integrity, etc.) of 3DP production should be considered and compared with one another in order to achieve the desired rheological characteristics. Besides, it is worth noting that the effect of print parameters on the interface or hardened characteristics are dependent on the material mixture. Moreover, the design mixture affects the rheological properties of concrete. In terms of 3DP concrete mix design parameters, it is important to bear in mind that the selection of mix

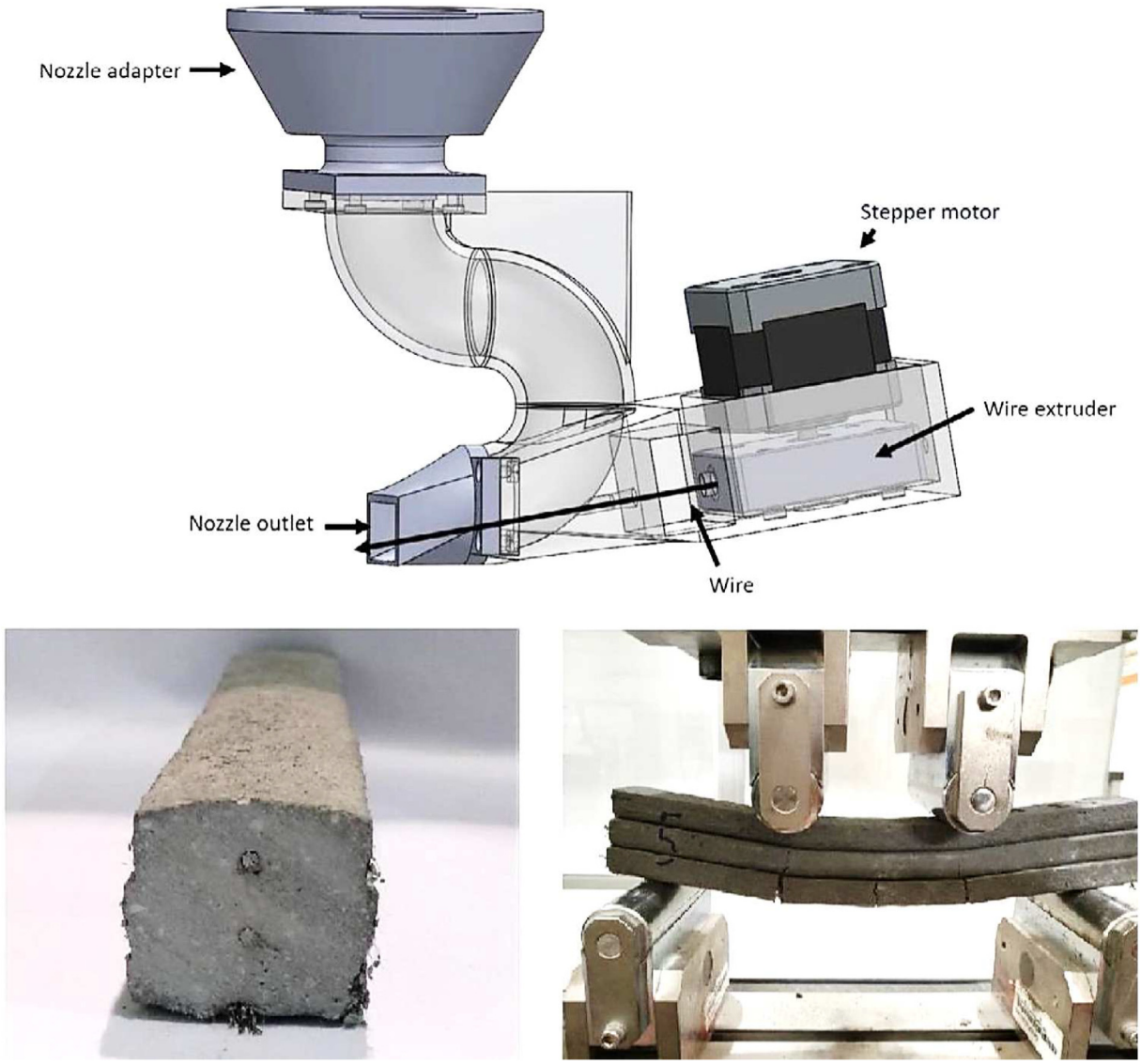

Fig. 31. Structural enhancement of 3DP-geopolymer composites by utilizing steel cable reinforcement [64].

ingredients and their proportions will be limited by the specific properties of the 3DP technology applied, as seen in Fig. 30. Another significant problem is adding reinforcement into 3DP technology for the building of reinforced concrete structures. Owing to the intrinsic operating process that does not require the use of formwork, the 3DP cementitious materials are not produced in the same method as traditional reinforced concrete construction. The traditional method of reinforced concrete construction is placing steel bars in a well-supported formwork and then filling them with concrete to make a structural concrete element. Another way to overcome the reinforcement difficulty is to use short fibers rather than standard steel bars. Only a few investigations have been conducted so far on the creation of 3DP fiber-reinforced GP composites. For instance, polypropylene fibers were used to avoid the material from shrinking and breaking during its plastic state, not to enhance its mechanical performance and ductility. The use of ultra-high-performance fiber-reinforced concrete to provide enough structural stability in cement-based materials can eliminate the need for traditional reinforcing steel in the 3DP [252]. The structural challenge may well be solved by 3DP-geopolymer composites with steel cable reinforcing nozzles, as illustrated in Fig. 31.

8. Conclusions

In this article, a comprehensive review of 3DP-geopolymer composites is performed. The conclusions drawn are as follows:

1. To ensure ideal printability, a balance between various types of fresh characteristics must be achieved, which can be tuned by modifying the mix proportions of geopolymers mostly by trial-and-error;
2. Because of the automatic layer deposition process, a strong interfacial bond is critical for enabling monolithic action in 3DP concrete;
3. Microwave heating following depositing can improve 3D printing geopolymer bond strength, and this heating system deployed at the print-head might be thought of as a viable set-on-demand approach for geopolymers;
4. Increased time between layers weakens the structure, although the influence of printing speed and nozzle standoff distance is better at lower values;
5. Owing to the layer-wise production method employed in concrete printing, the printed GPs demonstrated anisotropic

mechanical performance in comparison to the molded cast samples;
6. The activator's viscosity influenced the GP's resulting viscosity. Additionally, it was discovered that the viscosity and yield stress increase with the molar ratio. At a low molar ratio (1.8), the yield stress achieved was insufficient to preserve the geometry of the printed layers;
7. Clay's effect on fresh and hardened characteristics was highly dependent on the activator to binder and water to solid ratios utilized in the creation of the GP binders. Additionally, incorporating a small volume of nanoclay into the GP improved the essential rheological characteristics for 3DP applications. These improvements have been linked to the clay particles' flocculation properties;
8. Thixotropy, yield stress, and mechanical strength increased with increasing ground-granulated blast furnace slag (GGBFS) concentration due to its angular morphology and amorphous stages. Additionally, the introduction of GGBFS resulted in the formation of a stronger three-dimensional network, which has the ability to increase the ultimate strength of GPs owing to its amorphous phases. Whereas GGBFS did not significantly enhance the material's rheological behavior, it had an effect on the time-dependent structural build-up in the material by decreasing the workable time of the paste. As a result, its dosage in the mixture should be carefully monitored while keeping an adequate finish strength level;
9. The addition of silica fume (SF) was beneficial in reducing the yield stress and viscosity of the fresh phase mixtures. These advantages were attributable to the SF particles' large surface area and spherical form, which permitted smooth extrusion of the mix and demonstrated a good recovery behavior due to the shape preservation of the deposited filaments;
10. The use of hybrid reinforcement in printed GPs can help minimize cable slippage. This enhancement is related to the interaction between short polyvinyl alcohol (PVA) fibers and microcracks generated by the long steel cables being pulled out. Additionally, improving the flexural strength and fracture toughness of 3DP-geopolymer composites;
11. Because of the unique 3DP technique, the size of aggregate and type of fiber are frequently constrained, which may limit the development of tensile characteristics and reduce shrinkage resistance for 3D printing geopolymer;
12. One-part geopolymers [GPs] (a substitute green binder activated by solid activators) have the potential to have a lower ecological impact than ordinary Portland cement (OPC)-based mixtures;
13. To enhance the sustainability of 3D printing geopolymer, prospective effective mixes should include a small amount of silica fume and GGBFS, a large amount of fly ash (FA), solid or liquid activator, river sand, retarder, and thixotropic additive;
14. Finally, it is critical to highlight that the suggested criteria and test techniques for the characterization of printable GP at the fresh stage are highly reliant on the chemical components of the mix and the equipment used to study the characteristics. Any variation in one of these factors may lead to various findings, and therefore, a material limit may be set for a specific printing application.

9. Recommendations

In addition to the challenges mentioned in Section 10, recommendations for future studies are as follows:

1. Further study should be directed at developing a more detailed knowledge of the reaction processes in order to enhance the mechanical performance of the developed formulations. This enables the end-user to modify the rheological behavior by adding suitable additives to get the desired result;
2. Further research should be done to investigate the impacts of printing configuration, loading type, and fiber reinforcement;
3. More research into transport processes is needed to assess the long-term durability of 3DP geopolymer;
4. 3DP-geopolymers are still facing technical issues and will require coordinated research initiatives to advance a stable mechanism to be implemented at full scale;
5. Moreover, relevant guidelines and standards for 3DP procedures are required to guarantee that GP concrete can become a component of engineers' design toolbox and gain traction as a sustainable and robust alternative to OPC concrete building;
6. Developing a relationship between the equipment and operating procedures, the material rheological properties, and the 3DP-geopolymer end geometry. A critical area of research consideration is to help bridge the gap and develop a relationship between the production process and material characteristics, as well as the printed layer shape, in order to increase printing accuracy. Additionally, more accurate control will assist in avoiding overshooting and surface finishing issues. The developed correlation may also aid in resolving issues with the 3DP-geopolymer rheology design. The process could be made more acceptable for mixes with different rheological characteristics by adjusting the equipment and operating process;
7. Additional research is needed to produce a 3DP-geopolymer that cures at room temperature in order to broaden the usage of this eco-friendly material in 3DP concrete;
8. More study is required regarding the influence of optimal material selection on the flow characteristics during and after the extrusion;
9. To fully use the potential of different bonding materials and recycled materials in 3D concrete mixes, more research needs to be done;
10. Additional studies into the effects of different factors on the fresh and hardened properties of a 3DP-geopolymer-based on fly ash, metakaolin, and other waste materials for extrusion-based 3DP concrete are required. These factors include the type of activator, the type of sodium silicate sol, and the sodium silicate/sodium hydroxide sol ratio;
11. Despite the proposed solutions and assurances, automation of the operation and establishing mechanical interlocking without impacting the geometry stability of the bottom layers of 3DP concrete demand additional attention and study;
12. Further research is required to investigate the extrudability of 3DP concrete by modifying the material's rheology and the type of extrusion used;
13. Together with printability, the investigation into the environmental and economic impacts of large-scale 3DP is critical;
14. Durability and Drying shrinkage of 3D printing geopolymer must be explored further to enhance engineering applications.

Declaration of competing interest

The authors declare that they have no known competing financial interests or personal relationships that could have appeared to influence the work reported in this paper.

Acknowledgment

This research is conducted under the auspices of The Palestinian Quebec Science Bridge (PQSB).

References

[1] S. Lim, et al., Developments in construction-scale additive manufacturing processes, Autom. ConStruct. 21 (2012) 262–268.
[2] T.T. Le, et al., Hardened properties of high-performance printing concrete, Cement Concr. Res. 42 (3) (2012) 558–566.
[3] Y.W.D. Tay, et al., 3D printing trends in building and construction industry: a review, Virtual Phys. Prototyp. 12 (3) (2017) 261–276.
[4] S.M.A. Qaidi, et al., Rubberized geopolymer composites: a comprehensive review, Ceram. Int. 48 (17) (2022) 24234–24259.
[5] Y.I.A. Aisheh, Dawood Sulaiman Atrushi, Mahmoud H. Akeed, Shaker Qaidi, B.A. Tayeh, Influence of steel fibres and microsilica on the mechanical properties of ultra-high-performance geopolymer concrete (UHP-GPC), Case Stud Constr. Mater 17 (2022) e01245.
[6] F. Bos, et al., Additive manufacturing of concrete in construction: potentials and challenges of 3D concrete printing, Virtual Phys. Prototyp. 11 (3) (2016) 209–225.
[7] J.P. Brannon, et al., Teaching crystallography by determining small molecule structures and 3-D printing: an inorganic chemistry laboratory module, J. Chem. Educ. 97 (8) (2020) 2273–2279.
[8] M. Tramontin Souza, et al., Role of temperature in 3D printed geopolymers: evaluating rheology and buildability, Mater. Lett. 293 (2021), 129680.
[9] S. Muthukrishnan, S. Ramakrishnan, J. Sanjayan, Effect of microwave heating on interlayer bonding and buildability of geopolymer 3D concrete printing, Construct. Build. Mater. 265 (2020), 120786.
[10] G. Ma, et al., Micro-cable reinforced geopolymer composite for extrusion-based 3D printing, Mater. Lett. 235 (2019) 144–147.
[11] T. Wangler, et al., Digital concrete: a review, Cement Concr. Res. 123 (2019), 105780.
[12] Y.I.A. Aisheh, et al., Influence of polypropylene and steel fibers on the mechanical properties of ultra-high-performance fiber-reinforced geopolymer concrete, Case Stud. Constr. Mater. (2022), e01234.
[13] S.C. Paul, et al., A review of 3D concrete printing systems and materials properties: current status and future research prospects, Rapid Prototyp. J. 24 (4) (2018) 784–798.
[14] M.T. Marvila, et al., Performance of geopolymer tiles in high temperature and saturation conditions, Construct. Build. Mater. 286 (2021), 122994.
[15] V. Mechtcherine, et al., Extrusion-based additive manufacturing with cement-based materials—production steps, processes, and their underlying physics: a review, Cement Concr. Res. 132 (2020), 106037.
[16] Shaker M.A. Qaidi, B.A.T. Haytham, F. Isleem, Afonso R.G. de Azevedo, Hemn Unis Ahmed, Wael Emad, Sustainable utilization of red mud waste (bauxite residue) and slag for the production of geopolymer composites: a review, Case Stud. Constr. Mater. 16 (2022) e00994.
[17] S.M.A. Qaidi, et al., Engineering properties of sustainable green concrete incorporating eco-friendly aggregate of crumb rubber: a review, J. Clean. Prod. (2021), 129251.
[18] S.M.A. Qaidi, Y.S.S. Al-Kamaki, State-of-the-Art review: concrete made of recycled waste PET as fine aggregate, J. Donghua Univ. 23 (2) (2021) 412–429.
[19] C. Gosselin, et al., Large-scale 3D printing of ultra-high performance concrete—a new processing route for architects and builders, Mater. Des. 100 (2016) 102–109.
[20] J. Xiao, et al., Large-scale 3D printing concrete technology: current status and future opportunities, Cement Concr. Compos. 122 (2021), 104115.
[21] X. Han, et al., Experimental study on large-scale 3D printed concrete walls under axial compression, Autom. ConStruct. 133 (2022), 103993.
[22] T. Daungwilailuk, P. Pheinsusom, W. Pansuk, Uniaxial load testing of large-scale 3D-printed concrete wall and finite-element model analysis, Construct. Build. Mater. 275 (2021), 122039.
[23] S.M.A. Qaidi, Ultra-high-performance Fiber-Reinforced Concrete: Challenges, 2022.
[24] S.M.A. Qaidi, Ultra-high-performance Fiber-Reinforced Concrete: Applications, 2022.
[25] S.M.A. Qaidi, Ultra-high-performance Fiber-Reinforced Concrete: Cost Assessment, 2022.
[26] S. Qaidi, Behaviour of Concrete Made of Recycled Waste PET and Confined with CFRP Fabrics, 2021.
[27] H.U. Ahmed, et al., Compressive strength of geopolymer concrete composites: a systematic comprehensive review, analysis and modeling, European Journal of Environmental and Civil Engineering (2022) 1–46.
[28] X. He, et al., Mine tailings-based geopolymers: a comprehensive review, Ceram. Int. 48 (17) (2022) 24192–24212.
[29] A. Davidovits, Geopolymers: inorganic polymeric new materials, J. Therm. Anal. 37 (1991) 1633–1656.
[30] H.U. Ahmed, et al., Compressive strength of sustainable geopolymer concrete composites: a state-of-the-art review, Sustainability 13 (24) (2021), 13502.
[31] Y.I.A. Aisheh, et al., Influence of steel fibers and microsilica on the mechanical properties of ultra-high-performance geopolymer concrete (UHP-GPC), Case Stud. Constr. Mater. 17 (2022), e01245.
[32] F. Aslam, et al., Evaluating the influence of fly ash and waste glass on the characteristics of coconut fibers reinforced concrete, Struct. Concr. (2022).
[33] V. Mechtcherine, et al., 3D-printed steel reinforcement for digital concrete construction–Manufacture, mechanical properties and bond behaviour, Construct. Build. Mater. 179 (2018) 125–137.
[34] B.C. Mendes, et al., Application of eco-friendly alternative activators in alkali-activated materials: a review, J. Build. Eng. 35 (2021), 102010.
[35] M.T. Marvila, et al., Mechanical, physical and durability properties of activated alkali cement based on blast furnace slag as a function of% Na_2O, Case Stud. Constr. Mater. 15 (2021), e00723.
[36] H. Gökçe, M. Tuyan, M. Nehdi, Alkali-activated and geopolymer materials developed using innovative manufacturing techniques: a critical review, Construct. Build. Mater. 303 (2021), 124483.
[37] S.M.A. Qaidi, Ultra-high-performance Fiber-Reinforced Concrete: Durability Properties, 2022.
[38] S.M.A. Qaidi, Ultra-high-performance Fiber-Reinforced Concrete: Hardened Properties, 2022.
[39] S.M.A. Qaidi, Ultra-high-performance Fiber-Reinforced Concrete: Fresh Properties, 2022.
[40] S.M.A. Qaidi, Ultra-high-performance Fiber-Reinforced Concrete: Hydration and Microstructure, 2022.
[41] S.M.A. Qaidi, Ultra-high-performance Fiber-Reinforced Concrete: Mixture Design, 2022.
[42] S.M.A. Qaidi, Ultra-high-performance Fiber-Reinforced Concrete: Principles and Raw Materials, 2022.
[43] M. Amran, et al., 3D-printable alkali-activated concretes for building applications: a critical review, Construct. Build. Mater. 319 (2022), 126126.
[44] A. du Plessis, et al., Biomimicry for 3D concrete printing: a review and perspective, Addit. Manuf. 38 (2021), 101823.
[45] P. Zhang, et al., Fabrication and engineering properties of concretes based on geopolymers/alkali-activated binders-a review, J. Clean. Prod. 258 (2020), 120896.
[46] J.G. Sanjayan, A. Nazari, B. Nematollahi, 3D Concrete Printing Technology: Construction and Building Applications, Butterworth-Heinemann, 2019.
[47] A. Tibaut, D. Rebolj, M. Nekrep Perc, Interoperability requirements for automated manufacturing systems in construction, J. Intell. Manuf. 27 (1) (2016) 251–262.
[48] M. Xia, J. Sanjayan, Method of formulating geopolymer for 3D printing for construction applications, Mater. Des. 110 (2016) 382–390.
[49] R. Rael, V. San Fratello, Developing Concrete Polymer Building Components for 3D Printing, 2011.
[50] K. Wadher, et al., 3D printing in pharmaceuticals: an emerging technology full of challenges, Ann. Pharm. Fr. 79 (2) (2021) 107–118.
[51] G. Cesaretti, et al., Building components for an outpost on the lunar soil by means of a novel 3D printing technology, Acta Astronaut. 93 (2014) 430–450.
[52] H. Moon, et al., Strategy for D-shape assembly of ITER vacuum vessel sector #06 as applying 3D metrology, Fusion Eng. Des. 169 (2021), 112476.
[53] S. Lim, et al., Development of a Viable Concrete Printing Process, 2011.
[54] J. Zhang, B. Khoshnevis, Optimal machine operation planning for construction by Contour Crafting, Autom. ConStruct. 29 (2013) 50–67.
[55] G. Xu, et al., 3D reconstruction of AGS friction disk based on robust active-contour concentric conics, Measurement 188 (2022), 110582.
[56] L. Gajny, et al., Fast quasi-automated 3D reconstruction of lower limbs from low dose biplanar radiographs using statistical shape models and contour matching, Med. Eng. Phys. 101 (2022), 103769.
[57] R.A. Buswell, et al., A process classification framework for defining and describing Digital Fabrication with Concrete, Cement Concr. Res. 134 (2020), 106068.
[58] B. Nematollahi, M. Xia, J. Sanjayan, Current progress of 3D concrete printing technologies, in: ISARC. Proceedings of the International Symposium on Automation and Robotics in Construction, IAARC Publications, 2017.
[59] W. Wang, et al., Fresh and rheological characteristics of fiber reinforced concrete—a review, Construct. Build. Mater. 296 (2021), 123734.
[60] W. Lao, M. Li, T. Tjahjowidodo, Variable-geometry nozzle for surface quality enhancement in 3D concrete printing, Addit. Manuf. 37 (2021), 101638.
[61] H.G. Şahin, A. Mardani-Aghabaglou, Assessment of materials, design parameters and some properties of 3D printing concrete mixtures; a state-of-the-art review, Construct. Build. Mater. 316 (2022), 125865.
[62] J.H. Jo, et al., Development of a 3D printer for concrete structures: laboratory testing of cementitious materials, Int. J. Concr. Struct. Mater. 14 (1) (2020) 1–11.
[63] B. Panda, M.J. Tan, Rheological behavior of high volume fly ash mixtures containing micro silica for digital construction application, Mater. Lett. 237 (2019) 348–351.
[64] J.H. Lim, B. Panda, Q.-C. Pham, Improving flexural characteristics of 3D printed geopolymer composites with in-process steel cable reinforcement, Construct. Build. Mater. 178 (2018) 32–41.
[65] B. Panda, M.J. Tan, Experimental study on mix proportion and fresh properties of fly ash based geopolymer for 3D concrete printing, Ceram. Int. 44 (9) (2018) 10258–10265.

[66] B. Panda, C. Unluer, M.J. Tan, Investigation of the rheology and strength of geopolymer mixtures for extrusion-based 3D printing, Cement Concr. Compos. 94 (2018) 307–314.
[67] Y. Tao, et al., Mechanical and microstructural properties of 3D printable concrete in the context of the twin-pipe pumping strategy, Cement Concr. Compos. 125 (2022), 104324.
[68] A.D. Raval, C.G. Patel, Estimation of interface friction and concrete boundary layer for 3D printable concrete pumping, Mater. Today Proc. (2022).
[69] M.S. Choi, Y.J. Kim, J.K. Kim, Prediction of concrete pumping using various rheological models, Int. J. Concr. Struct. Mater. 8 (4) (2014) 269–278.
[70] S.H. Kwon, et al., State of the art on prediction of concrete pumping, Int. J. Concr. Struct. Mater. 10 (3) (2016) 75–85.
[71] F.P. Bos, et al., Juxtaposing fresh material characterisation methods for buildability assessment of 3D printable cementitious mortars, Cement Concr. Compos. 120 (2021), 104024.
[72] H. Alghamdi, S.A. Nair, N. Neithalath, Insights into material design, extrusion rheology, and properties of 3D-printable alkali-activated fly ash-based binders, Mater. Des. 167 (2019), 107634.
[73] B. Panda, C. Unluer, M.J. Tan, Extrusion and rheology characterization of geopolymer nanocomposites used in 3D printing, Compos. B Eng. 176 (2019), 107290.
[74] M. Palacios, F. Puertas, Effect of superplasticizer and shrinkage-reducing admixtures on alkali-activated slag pastes and mortars, Cement Concr. Res. 35 (7) (2005) 1358–1367.
[75] R.A. Buswell, et al., 3D printing using concrete extrusion: a roadmap for research, Cement Concr. Res. 112 (2018) 37–49.
[76] M. Khan, Mix suitable for concrete 3D printing: a review, Mater. Today Proc. 32 (2020) 831–837.
[77] C. Zhang, et al., Mix design concepts for 3D printable concrete: a review, Cement Concr. Compos. 122 (2021), 104155.
[78] R.J.M. Wolfs, F.P. Bos, T.A.M. Salet, Correlation between destructive compression tests and non-destructive ultrasonic measurements on early age 3D printed concrete, Construct. Build. Mater. 181 (2018) 447–454.
[79] T.D. Ngo, et al., Additive manufacturing (3D printing): a review of materials, methods, applications and challenges, Compos. B Eng. 143 (2018) 172–196.
[80] H. Yue, et al., Investigation on applicability of spherical electric arc furnace slag as fine aggregate in superplasticizer-free 3D printed concrete, Construct. Build. Mater. 319 (2022), 126104.
[81] S. Geetha, M. Selvakumar, S.M. Lakshmi, 3D concrete printing matrix reinforced with Geogrid, Mater. Today Proc. 49 (2022) 1443–1447.
[82] M. Batikha, et al., 3D concrete printing for sustainable and economical construction: a comparative study, Autom. ConStruct. 134 (2022), 104087.
[83] S.M.A. Qaidi, PET-Concrete Confinement with CFRP, 2021.
[84] S.M.A. Qaidi, PET-Concrete, 2021.
[85] S.M.A. Qaidi, Behavior of Concrete Made of Recycled PET Waste and Confined with CFRP Fabrics, College of Engineering, University of Duhok, 2021.
[86] A. Mansi, et al., The impact of nano clay on normal and high-performance concrete characteristics: a review, in: IOP Conference Series: Earth and Environmental Science 961, IOP Publishing, 2022, p. 012085.
[87] R.A. Buswell, et al., Freeform construction: mega-scale rapid manufacturing for construction, Autom. ConStruct. 16 (2) (2007) 224–231.
[88] Y. Han, et al., Environmental and economic assessment on 3D printed buildings with recycled concrete, J. Clean. Prod. 278 (2021), 123884.
[89] A. Cicione, et al., An experimental study of the behavior of 3D printed concrete at elevated temperatures, Fire Saf. J. 120 (2021), 103075.
[90] Y. Weng, et al., Comparative economic, environmental and productivity assessment of a concrete bathroom unit fabricated through 3D printing and a precast approach, J. Clean. Prod. 261 (2020), 121245.
[91] F.A. Jawad Ahmad, Rebeca Martinez-Garcia, Jesús de-Prado-Gil, Shaker M.A. Qaidi, Ameni Brahmia, Effects of waste glass and waste marble on mechanical and durability performance of concrete, Sci. Rep. 11 (1) (2021), 21525.
[92] Ibrahim Almeshal, M.M. Al-Tayeb, S.M.A. Qaidi, B.H. Abu Bakar, B.A. Tayeh, Mechanical properties of eco-friendly cements-based glass powder in aggressive medium, Mater. Today Proc. 58 (2022) 1582–1587.
[93] R.H. Faraj, et al., Performance of self-compacting mortars modified with nanoparticles: a systematic review and modeling, Clean. Mater. 4 (2022), 100086.
[94] Faraj, R.H., et al., Cleaner Materials.
[95] S.N. Ahmed, et al., Thermal conductivity and hardened behavior of eco-friendly concrete incorporating waste polypropylene as fine aggregate, Mater. Today Proc. (2022).
[96] V.N. Nerella, M. Krause, V. Mechtcherine, Direct printing test for buildability of 3D-printable concrete considering economic viability, Autom. ConStruct. 109 (2020), 102986.
[97] A.S. Alchaar, A.K. Al-Tamimi, Mechanical properties of 3D printed concrete in hot temperatures, Construct. Build. Mater. 266 (2021) 120991.
[98] J. Sanjayan, R. Jayathilakage, P. Rajeev, Vibration induced active rheology control for 3D concrete printing, Cement Concr. Res. 140 (2021), 106293.
[99] Ahmed, H.U., et al., Compressive strength of geopolymer concrete modified with nano-silica: experimental and modeling investigations. Case Stud. Constr. Mater., 2022(2): p. e01036.
[100] H.U. Ahmed, et al., Compressive strength of sustainable geopolymer concrete composites: a state-of-the-art review, Sustainability 13 (24) (2021), 13502.
[101] V. Nerella, et al., Strain-based approach for measuring structural build-up of cement pastes in the context of digital construction, Cement Concr. Res. 115 (2019) 530–544.
[102] G. Moelich, P. Kruger, R. Combrinck, The effect of restrained early age shrinkage on the interlayer bond and durability of 3D printed concrete, J. Build. Eng. 43 (2021), 102857.
[103] R.H. Faraj, A.A. Mohammed, K.M. Omer, Self-compacting concrete composites modified with nanoparticles: a comprehensive review, analysis and modeling, J. Build. Eng. (2022), 104170.
[104] T.T. Le, et al., Mix design and fresh properties for high-performance printing concrete, Mater. Struct. 45 (8) (2012) 1221–1232.
[105] M.T. Souza, et al., 3D printed concrete for large-scale buildings: an overview of rheology, printing parameters, chemical admixtures, reinforcements, and economic and environmental prospects, J. Build. Eng. 32 (2020), 101833.
[106] G. Ma, L. Wang, A critical review of preparation design and workability measurement of concrete material for largescale 3D printing, Front. Struct. Civ. Eng. 12 (3) (2018) 382–400.
[107] Y. Zhang, et al., Rheological and harden properties of the high-thixotropy 3D printing concrete, Construct. Build. Mater. 201 (2019) 278–285.
[108] B. Panda, et al., Improving the 3D printability of high volume fly ash mixtures via the use of nano attapulgite clay, Compos. B Eng. 165 (2019) 75–83.
[109] D.G. Snelson, S. Wild, M. O'Farrell, Heat of hydration of Portland cement–metakaolin–fly ash (PC–MK–PFA) blends, Cement Concr. Res. 38 (6) (2008) 832–840.
[110] A. Mardani-Aghabaglou, et al., Effect of cement fineness on properties of cementitious materials containing high range water reducing admixture, J. Green Build. 12 (1) (2017) 142–167.
[111] J. Ye, et al., Fresh and anisotropic-mechanical properties of 3D printable ultra-high ductile concrete with crumb rubber, Compos. B Eng. 211 (2021), 108639.
[112] S. Yu, et al., Anisotropic microstructure dependent mechanical behavior of 3D-printed basalt fiber-reinforced thermoplastic composites, Compos. B Eng. 224 (2021), 109184.
[113] K. Wan, et al., 3D full field study of drying shrinkage of foam concrete, Cement Concr. Compos. 82 (2017) 217–226.
[114] Y. Chen, et al., Application of 3D-DIC to characterize the effect of aggregate size and volume on non-uniform shrinkage strain distribution in concrete, Cement Concr. Compos. 86 (2018) 178–189.
[115] A. Azevedo, et al., Rheology, hydration, and microstructure of Portland cement pastes produced with ground açaí fibers, Appl. Sci. 11 (7) (2021) 3036.
[116] A.R. de Azevedo, et al., Natural fibers as an alternative to synthetic fibers in reinforcement of geopolymer matrices: a comparative review, Polymers 13 (15) (2021) 2493.
[117] M.T. Marvila, et al., Materials for production of high and ultra-high performance concrete: review and perspective of possible novel materials, Materials 14 (15) (2021) 4304.
[118] N. Labonnote, et al., Additive construction: state-of-the-art, challenges and opportunities, Autom. ConStruct. 72 (2016) 347–366.
[119] G. De Schutter, et al., Vision of 3D printing with concrete–technical, economic and environmental potentials, Cement Concr. Res. 112 (2018) 25–36.
[120] A.R. De Azevedo, et al., Circular economy and durability in geopolymers ceramics pieces obtained from glass polishing waste, Int. J. Appl. Ceram. Technol. 18 (6) (2021) 1891–1900.
[121] J. Orr, Flexible Formwork for Concrete Structures, University of Bath, 2012.
[122] B.G. de Soto, et al., Productivity of digital fabrication in construction: cost and time analysis of a robotically built wall, Autom. ConStruct. 92 (2018) 297–311.
[123] F.P. Bos, et al., The realities of additively manufactured concrete structures in practice, Cement Concr. Res. 156 (2022), 106746.
[124] S. Cai, et al., Construction automation and robotics for high-rise buildings over the past decades: a comprehensive review, Adv. Eng. Inf. 42 (2019), 100989.
[125] E. Brehm, Robots for masonry construction–Status quo and thoughts for the German market, Mauerwerk 23 (2) (2019) 87–94.
[126] E. Grigoryan, M. Semenova, Automation of the construction process by using a hinged robot with interchangeable nozzles, Mater. Today Proc. 30 (2020) 380–387.
[127] E. Grigoryan, A. Babanina, K. Kulakov, Automation of the construction process by using a hinged robot with interchangeable nozzles, in: Energy Management of Municipal Transportation Facilities and Transport, Springer, 2019.
[128] I. Attah, R. Etim, I. Usanga, Potentials of cement kiln dust and rice husk ash blend on strength of tropical soil for sustainable road construction material, in: IOP Conference Series: Materials Science and Engineering, IOP Publishing, 2021.
[129] M. Adaloudis, J. Bonnin Roca, Sustainability tradeoffs in the adoption of 3D Concrete Printing in the construction industry, J. Clean. Prod. 307 (2021), 127201.
[130] B. Khoshnevis, Automated construction by contour crafting–related robotics and information technologies, Autom. ConStruct. 13 (1) (2004) 5–19.
[131] I. Oberti, F. Plantamura, Is 3D printed house sustainable?, in: Proceedings of International Conference CISBAT 2015 Future Buildings and Districts Sustainability from Nano to Urban Scale LESO-PB, EPFL, 2015.

[132] B. Nematollahi, et al., Hardened properties of 3D printable 'one-part'geopolymer for construction applications, in: RILEM International Conference on Concrete and Digital Fabrication, Springer, 2018.
[133] M. Xia, B. Nematollahi, J. Sanjayan, Printability, accuracy and strength of geopolymer made using powder-based 3D printing for construction applications, Autom. ConStruct. 101 (2019) 179–189.
[134] G. Ma, et al., Mechanical anisotropy of aligned fiber reinforced composite for extrusion-based 3D printing, Construct. Build. Mater. 202 (2019) 770–783.
[135] G. Ma, Z. Li, L. Wang, Printable properties of cementitious material containing copper tailings for extrusion based 3D printing, Construct. Build. Mater. 162 (2018) 613–627.
[136] R. Jayathilakage, P. Rajeev, J. Sanjayan, Yield stress criteria to assess the buildability of 3D concrete printing, Construct. Build. Mater. 240 (2020), 117989.
[137] K. Federowicz, et al., Effect of curing methods on shrinkage development in 3D-printed concrete, Materials 13 (11) (2020) 2590.
[138] X. Zhang, et al., Large-scale 3D printing by a team of mobile robots, Autom. ConStruct. 95 (2018) 98–106.
[139] R. Wolfs, F. Bos, T. Salet, Early age mechanical behaviour of 3D printed concrete: numerical modelling and experimental testing, Cement Concr. Res. 106 (2018) 103–116.
[140] D. Asprone, et al., 3D printing of reinforced concrete elements: technology and design approach, Construct. Build. Mater. 165 (2018) 218–231.
[141] G. Ji, et al., A 3D printed ready-mixed concrete power distribution substation: materials and construction technology, Materials 12 (9) (2019) 1540.
[142] A. Kazemian, et al., Cementitious materials for construction-scale 3D printing: laboratory testing of fresh printing mixture, Construct. Build. Mater. 145 (2017) 639–647.
[143] F. Tahmasebinia, et al., Criteria development for sustainable construction manufacturing in construction industry 4.0: theoretical and laboratory investigations, Construct. Innov. 20 (3) (2020) 379–400.
[144] C. Zhang, et al., Design of 3D printable concrete based on the relationship between flowability of cement paste and optimum aggregate content, Cement Concr. Compos. 104 (2019), 103406.
[145] A.V. Rahul, et al., 3D printable concrete with natural and recycled coarse aggregates: rheological, mechanical and shrinkage behaviour, Cement Concr. Compos. 125 (2022), 104311.
[146] D. Jiao, C. Shi, G. De Schutter, Magneto-rheology control in 3D concrete printing: a rheological attempt, Mater. Lett. 309 (2022), 131374.
[147] S. Cho, et al., Foam stability of 3D printable foamed concrete, J. Build. Eng. 47 (2022), 103884.
[148] K.M. Claeson, D.J. Ward, C.J. Underwood, 3D digital imaging of a concretion-preserved batoid (chondrichthyes, elasmobranchii) from the turonian (upper cretaceous) of Morocco, Comptes Rendus Palevol 9 (6) (2010) 283–287.
[149] A.G. Marangoni, L.H. Wesdorp, Structure and Properties of Fat Crystal Networks, CRC Press, 2012.
[150] Q.M. Zaigham Zia, et al., Cross diffusion and exponential space dependent heat source impacts in radiated three-dimensional (3D) flow of Casson fluid by heated surface, Results Phys. 8 (2018) 1275–1282.
[151] B.J. Gireesha, et al., Nonlinear 3D flow of Casson-Carreau fluids with homogeneous–heterogeneous reactions: a comparative study, Results Phys. 7 (2017) 2762–2770.
[152] D. Marchon, et al., Hydration and rheology control of concrete for digital fabrication: potential admixtures and cement chemistry, Cement Concr. Res. 112 (2018) 96–110.
[153] S.C. Paul, et al., Fresh and hardened properties of 3D printable cementitious materials for building and construction, Arch. Civ. Mech. Eng. 18 (1) (2018) 311–319.
[154] N. Roussel, Rheological requirements for printable concretes, Cement Concr. Res. 112 (2018) 76–85.
[155] L. Reiter, et al., The role of early age structural build-up in digital fabrication with concrete, Cement Concr. Res. 112 (2018) 86–95.
[156] A. Favier, et al., Flow properties of MK-based geopolymer pastes. A comparative study with standard Portland cement pastes, Soft Matter 10 (8) (2014) 1134–1141.
[157] G. Bai, et al., 3D printing eco-friendly concrete containing under-utilised and waste solids as aggregates, Cement Concr. Compos. 120 (2021), 104037.
[158] F. Heidarnezhad, Q. Zhang, Shotcrete based 3D concrete printing: state of art, challenges, and opportunities, Construct. Build. Mater. 323 (2022), 126545.
[159] M. Jolin, et al., Understanding the Pumpability of Concrete, 2009.
[160] S. Al-Qutaifi, A. Nazari, A. Bagheri, Mechanical properties of layered geopolymer structures applicable in concrete 3D-printing, Construct. Build. Mater. 176 (2018) 690–699.
[161] Y. Zhang, et al., Fresh properties of a novel 3D printing concrete ink, Construct. Build. Mater. 174 (2018) 263–271.
[162] Y. Weng, et al., Design 3D printing cementitious materials via Fuller Thompson theory and Marson-Percy model, Construct. Build. Mater. 163 (2018) 600–610.
[163] B. Panda, et al., Measurement of tensile bond strength of 3D printed geopolymer mortar, Measurement 113 (2018) 108–116.
[164] V.N. Nerella, S. Hempel, V. Mechtcherine, Effects of layer-interface properties on mechanical performance of concrete elements produced by extrusion-based 3D-printing, Construct. Build. Mater. 205 (2019) 586–601.
[165] E.-H. Yang, Y. Yang, V.C. Li, Use of high volumes of fly ash to improve ECC mechanical properties and material greenness, ACI Mater. J. 104 (6) (2007) 620.
[166] E. Jamieson, et al., Comparison of embodied energies of ordinary Portland cement with Bayer-derived geopolymer products, J. Clean. Prod. 99 (2015) 112–118.
[167] G. Habert, J.D.E. De Lacaillerie, N. Roussel, An environmental evaluation of geopolymer based concrete production: reviewing current research trends, J. Clean. Prod. 19 (11) (2011) 1229–1238.
[168] T. Wangler, R.J. Flatt, in: First RILEM International Conference on Concrete and Digital Fabrication–Digital Concrete 2018, vol. 19, Springer, 2018.
[169] M. Amran, et al., Fiber-reinforced alkali-activated concrete: a review, J. Build. Eng. 45 (2022), 103638.
[170] I. Agustí-Juan, G. Habert, Environmental design guidelines for digital fabrication, J. Clean. Prod. 142 (2017) 2780–2791.
[171] Y. He, et al., Energy-saving potential of 3D printed concrete building with integrated living wall, Energy Build. 222 (2020), 110110.
[172] S. Yang, et al., Novel proposal to overcome insulation limitations due to nonlinear structures using 3D printing: hybrid heat-storage system, Energy Build. 197 (2019) 177–187.
[173] X. Li, Y. Zhu, Z. Zhang, An LCA-based environmental impact assessment model for construction processes, Build. Environ. 45 (3) (2010) 766–775.
[174] L. Ma, et al., Effect of drying environment on mechanical properties, internal RH and pore structure of 3D printed concrete, Construct. Build. Mater. 315 (2022), 125731.
[175] M. Liu, et al., 3D meso-scale modelling of the bonding failure between corroded ribbed steel bar and concrete, Eng. Struct. 256 (2022), 113939.
[176] S.H. Bong, et al., Ambient temperature cured 'just-add-water' geopolymer for 3D concrete printing applications, Cement Concr. Compos. 121 (2021) 104060.
[177] S.-W. Kim, et al., Mechanical properties and eco-efficiency of steel fiber reinforced alkali-activated slag concrete, Materials 8 (11) (2015) 7309–7321.
[178] K. Yang, J. Song, K. Song, CO2 reduction assessment of alkali-activated concrete based on Korean life-cycle inventory database, in: A. Nazari, J.G. Sanjayan (Eds.), Handbook of Low Carbon Concrete, 2016, pp. 139–157.
[179] M. Fawer, M. Concannon, W. Rieber, Life cycle inventories for the production of sodium silicates, Int. J. Life Cycle Assess. 4 (4) (1999) 207–212.
[180] P. Rein, The carbon footprint of sugar, Proc. Int. Soc. Sugar Cane Technol. (2010).
[181] A.U. Rehman, J.-H. Kim, 3D concrete printing: a systematic review of rheology, mix designs, mechanical, microstructural, and durability characteristics, Materials 14 (14) (2021) 3800.
[182] M. Palacios, et al., Influence of the alkaline solution and temperature on the rheology and reactivity of alkali-activated fly ash pastes, Cement Concr. Compos. 95 (2019) 277–284.
[183] S. Muthukrishnan, et al., Fresh properties of cementitious materials containing rice husk ash for construction 3D printing, J. Mater. Civ. Eng. 32 (8) (2020) 04020195.
[184] E. Lloret, et al., Complex concrete structures: merging existing casting techniques with digital fabrication, Comput. Aided Des. 60 (2015) 40–49.
[185] L. Reiter, et al., Setting on demand for digital concrete–principles, measurements, chemistry, validation, Cement Concr. Res. 132 (2020), 106047.
[186] R.J.M. Wolfs, F.P. Bos, T.A.M. Salet, Triaxial compression testing on early age concrete for numerical analysis of 3D concrete printing, Cement Concr. Compos. 104 (2019), 103344.
[187] A. Suiker, Mechanical performance of wall structures in 3D printing processes: theory, design tools and experiments, Int. J. Mech. Sci. 137 (2018) 145–170.
[188] V. Lesovik, et al., Four-component high-strength polymineral binders, Construct. Build. Mater. 316 (2022), 125934.
[189] A. Tripathi, S.A.O. Nair, N. Neithalath, A comprehensive analysis of buildability of 3D-printed concrete and the use of bi-linear stress-strain criterion-based failure curves towards their prediction, Cement Concr. Compos. 128 (2022), 104424.
[190] A.S.J. Suiker, et al., Elastic buckling and plastic collapse during 3D concrete printing, Cement Concr. Res. 135 (2020), 106016.
[191] J. Kruger, S. Zeranka, G. van Zijl, 3D concrete printing: a lower bound analytical model for buildability performance quantification, Autom. ConStruct. 106 (2019), 102904.
[192] J. Kruger, et al., 3D concrete printer parameter optimisation for high rate digital construction avoiding plastic collapse, Compos. B Eng. 183 (2020), 107660.
[193] Y. Yang, et al., 3D-printing ultra-high performance fiber-reinforced concrete under triaxial confining loads, Addit. Manuf. 50 (2022), 102568.
[194] Z. Tang, F. Huang, H. Peng, Effect of 3D roughness characteristics on bonding behaviors between concrete substrate and asphalt overlay, Construct. Build. Mater. 270 (2021), 121386.
[195] V. Lesovik, et al., 3D-Printed mortars with combined steel and polypropylene fibers, Fibers 9 (12) (2021) 79.
[196] G. Gelardi, R. Flatt, Working mechanisms of water reducers and superplasticizers, in: Science and Technology of Concrete Admixtures, Elsevier, 2016, pp. 257–278.
[197] V. Nguyen-Van, et al., Performance of concrete beam reinforced with 3D printed Bioinspired primitive scaffold subjected to three-point bending, Autom. ConStruct. 134 (2022), 104060.

[198] K. Khayat, N. Mikanovic, Viscosity-enhancing admixtures and the rheology of concrete, in: Understanding the Rheology of Concrete, Elsevier, 2012, pp. 209–228.
[199] M. Palacios, R. Flatt, Working mechanism of viscosity-modifying admixtures, in: Science and Technology of Concrete Admixtures, Elsevier, 2016, pp. 415–432.
[200] T. Voigt, et al., Using fly ash, clay, and fibers for simultaneous improvement of concrete green strength and consolidatability for slip-form pavement, J. Mater. Civ. Eng. 22 (2) (2010) 196–206.
[201] H. Alghamdi, N. Neithalath, Synthesis and characterization of 3D-printable geopolymeric foams for thermally efficient building envelope materials, Cement Concr. Compos. 104 (2019), 103377.
[202] D. Marchon, R. Flatt, Impact of chemical admixtures on cement hydration, in: Science and Technology of Concrete Admixtures, Elsevier, 2016, pp. 279–304.
[203] D. Marchon, et al., Molecular and submolecular scale effects of comb-co-polymers on tri-calcium silicate reactivity: toward molecular design, J. Am. Ceram. Soc. 100 (3) (2017) 817–841.
[204] G. Gelardi, et al., Chemistry of chemical admixtures, in: Science and Technology of Concrete Admixtures, Elsevier, 2016, pp. 149–218.
[205] S. Ramakrishnan, et al., Concrete 3D printing of lightweight elements using hollow-core extrusion of filaments, Cement Concr. Compos. 123 (2021), 104220.
[206] S. Muthukrishnan, S. Ramakrishnan, J. Sanjayan, Effect of alkali reactions on the rheology of one-part 3D printable geopolymer concrete, Cement Concr. Compos. 116 (2021), 103899.
[207] B. Panda, et al., Investigation of the properties of alkali-activated slag mixes involving the use of nanoclay and nucleation seeds for 3D printing, Compos. B Eng. 186 (2020), 107826.
[208] B. Nematollahi, et al., Digital fabrication of 'just-add-water'geopolymers: effects of curing condition and print-time interval, in: RILEM International Conference on Concrete and Digital Fabrication, Springer, 2020.
[209] B. Panda, et al., Synthesis and characterization of one-part geopolymers for extrusion based 3D concrete printing, J. Clean. Prod. 220 (2019) 610–619.
[210] M. Romagnoli, et al., Rheological characterization of fly ash-based suspensions, Construct. Build. Mater. 65 (2014) 526–534.
[211] F. Puertas, C. Varga, M. Alonso, Rheology of alkali-activated slag pastes. Effect of the nature and concentration of the activating solution, Cement Concr. Compos. 53 (2014) 279–288.
[212] M.V. Tran, Y.T.H. Cu, C.V.H. Le, Rheology and shrinkage of concrete using polypropylene fiber for 3D concrete printing, J. Build. Eng. 44 (2021), 103400.
[213] K. Kondepudi, K.V.L. Subramaniam, Formulation of alkali-activated fly ash-slag binders for 3D concrete printing, Cement Concr. Compos. 119 (2021), 103983.
[214] M. Chougan, et al., The influence of nano-additives in strengthening mechanical performance of 3D printed multi-binder geopolymer composites, Construct. Build. Mater. 250 (2020), 118928.
[215] C. Sun, et al., 3D extrusion free forming of geopolymer composites: materials modification and processing optimization, J. Clean. Prod. 258 (2020), 120986.
[216] A. Rahul, et al., 3D printable concrete: mixture design and test methods, Cement Concr. Compos. 97 (2019) 13–23.
[217] H. Lee, W. Kim, J. Moon, An experimental study of mortar rheology for 3D printing extruder, Proc. Korea Concr. Inst. Korea 29 (2) (2017).
[218] D.-W. Zhang, et al., The study of the structure rebuilding and yield stress of 3D printing geopolymer pastes, Construct. Build. Mater. 184 (2018) 575–580.
[219] J. Zhong, et al., 3D printing strong and conductive geo-polymer nanocomposite structures modified by graphene oxide, Carbon 117 (2017) 421–426.
[220] G. Franchin, et al., Direct ink writing of geopolymeric inks, J. Eur. Ceram. Soc. 37 (6) (2017) 2481–2489.
[221] B. Panda, et al., Additive manufacturing of geopolymer for sustainable built environment, J. Clean. Prod. 167 (2017) 281–288.
[222] C. Bai, et al., High-porosity geopolymer foams with tailored porosity for thermal insulation and wastewater treatment, J. Mater. Res. 32 (17) (2017) 3251–3259.
[223] G. Franchin, et al., Removal of ammonium from wastewater with geopolymer sorbents fabricated via additive manufacturing, Mater. Des. 195 (2020), 109006.
[224] Y. Huang, C. Wan, Controllable fabrication and multifunctional applications of graphene/ceramic composites, J. Adv. Ceram. 9 (3) (2020) 271–291.
[225] Y. Su, et al., Composite structural modeling and tensile mechanical behavior of graphene reinforced metal matrix composites, Sci. China Mater. 61 (1) (2018) 112–124.
[226] S. Stankovich, et al., Graphene-based composite materials, Nature 442 (7100) (2006) 282–286.
[227] X. Huang, et al., Graphene-based composites, Chem. Soc. Rev. 41 (2) (2012) 666–686.
[228] W.-J. Long, et al., Rheology and buildability of sustainable cement-based composites containing micro-crystalline cellulose for 3D-printing, J. Clean. Prod. 239 (2019), 118054.
[229] Y. Weng, et al., Feasibility study on sustainable magnesium potassium phosphate cement paste for 3D printing, Construct. Build. Mater. 221 (2019) 595–603.
[230] Q. Sun, et al., Synthesis and characterization of a geopolymer/hexagonal-boron nitride composite for free forming 3D extrusion-based printing, Appl. Clay Sci. 199 (2020), 105870.
[231] S. Pilehvar, et al., Investigation of severe lunar environmental conditions on the physical and mechanical properties of lunar regolith geopolymers, J. Mater. Res. Technol. 11 (2021) 1506–1516.
[232] M.T. Souza, et al., Role of temperature in 3D printed geopolymers: evaluating rheology and buildability, Mater. Lett. 293 (2021), 129680.
[233] S.H. Bong, et al., Effect of wollastonite micro-fiber addition on properties of 3D-printable 'just-add-Water' Geopolymers, in: RILEM International Conference on Concrete and Digital Fabrication, Springer, 2020.
[234] M. Chougan, et al., Investigation of additive incorporation on rheological, microstructural and mechanical properties of 3D printable alkali-activated materials, Mater. Des. 202 (2021), 109574.
[235] J. Archez, et al., Adaptation of the geopolymer composite formulation binder to the shaping process, Mater. Today Commun. 25 (2020), 101501.
[236] R. Comminal, et al., Modelling of 3D concrete printing based on computational fluid dynamics, Cement Concr. Res. 138 (2020), 106256.
[237] B. Zareiyan, B. Khoshnevis, Effects of interlocking on interlayer adhesion and strength of structures in 3D printing of concrete, Autom. ConStruct. 83 (2017) 212–221.
[238] Y. Zhang, et al., Relationship between water transport behaviour and interlayer voids of 3D printed concrete, Construct. Build. Mater. 326 (2022), 126731.
[239] M. van den Heever, et al., Evaluating the effects of porosity on the mechanical properties of extrusion-based 3D printed concrete, Cement Concr. Res. 153 (2022), 106695.
[240] A. Singh, et al., Mechanical and macrostructural properties of 3D printed concrete dosed with steel fibers under different loading direction, Construct. Build. Mater. 323 (2022), 126616.
[241] C. Liu, et al., Effect of sulphoaluminate cement on fresh and hardened properties of 3D printing foamed concrete, Compos. B Eng. 232 (2022), 109619.
[242] G. Ji, et al., Effects of extrusion parameters on properties of 3D printing concrete with coarse aggregates, Construct. Build. Mater. 325 (2022), 126740.
[243] Y. Chen, et al., A review of printing strategies, sustainable cementitious materials and characterization methods in the context of extrusion-based 3D concrete printing, J. Build. Eng. 45 (2022), 103599.
[244] Y.W.D. Tay, et al., Time gap effect on bond strength of 3D-printed concrete, Virtual Phys. Prototyp. 14 (1) (2019) 104–113.
[245] V. Markin, et al., 3D-printing with foam concrete: from material design and testing to application and sustainability, J. Build. Eng. 43 (2021), 102870.
[246] J. Kruger, A. du Plessis, G. van Zijl, An investigation into the porosity of extrusion-based 3D printed concrete, Addit. Manuf. 37 (2021), 101740.
[247] B. Panda, et al., Bond strength in 3D printed geopolymer mortar, in: RILEM International Conference on Concrete and Digital Fabrication, Springer, 2018.
[248] M. Xia, B. Nematollahi, J. Sanjayan, Compressive strength and dimensional accuracy of portland cement mortar made using powder-based 3D printing for construction applications, in: RILEM International Conference on Concrete and Digital Fabrication, Springer, 2018.
[249] C. Ma, et al., Properties and characterization of green one-part geopolymer activated by composite activators, J. Clean. Prod. 220 (2019) 188–199.
[250] M. Xia, B. Nematollahi, J. Sanjayan, Influence of binder saturation level on compressive strength and dimensional accuracy of powder-based 3D printed geopolymer, in: Materials Science Forum, Trans Tech Publ, 2018.
[251] B. Panda, S.C. Paul, M.J. Tan, Anisotropic mechanical performance of 3D printed fiber reinforced sustainable construction material, Mater. Lett. 209 (2017) 146–149.
[252] A.R. Arunothayan, et al., Development of 3D-printable ultra-high performance fiber-reinforced concrete for digital construction, Construct. Build. Mater. 257 (2020), 119546.
[253] B. Nematollahi, et al., Effect of polypropylene fiber addition on properties of geopolymers made by 3D printing for digital construction, Materials 11 (12) (2018) 2352.
[254] S.H. Bong, et al., Method of optimisation for ambient temperature cured sustainable geopolymers for 3D printing construction applications, Materials 12 (6) (2019) 902.
[255] D.G. Soltan, V.C. Li, A self-reinforced cementitious composite for building-scale 3D printing, Cement Concr. Compos. 90 (2018) 1–13.
[256] V.C. Li, et al., On the emergence of 3D printable engineered, strain hardening cementitious composites (ECC/SHCC), Cement Concr. Res. 132 (2020), 106038.
[257] S. Naderi, M. Zhang, A novel framework for modelling the 3D mesostructure of steel fibre reinforced concrete, Comput. Struct. 234 (2020), 106251.
[258] L. Gebhard, et al., Structural behaviour of 3D printed concrete beams with various reinforcement strategies, Eng. Struct. 240 (2021), 112380.
[259] S. Chaves Figueiredo, et al., Mechanical behavior of printed strain hardening cementitious composites, Materials 13 (10) (2020) 2253.
[260] Z.-X. Li, Y. Gao, Q. Zhao, A 3D flexure–shear fiber element for modeling the seismic behavior of reinforced concrete columns, Eng. Struct. 117 (2016) 372–383.
[261] D. Gao, et al., An inverse analysis method for multi-linear tensile stress-crack opening relationship of 3D/4D/5D steel fiber reinforced concrete, Construct. Build. Mater. 309 (2021), 125074.

[262] K. Bilisik, H. Ozdemir, Multiaxis three dimensional (3D) carbon and basalt preforms/cementitious matrix concretes: experimental study on fiber orientation and placement by panel test, Construct. Build. Mater. 271 (2021), 121863.
[263] K. Bilisik, H. Ozdemir, Multiaxis three-dimensional (3D) glass fiber preform/cementitious matrix concrete composites: experimental characterizations by panel test, Cement Concr. Compos. 119 (2021), 104020.
[264] K. Yu, et al., 3D-printable engineered cementitious composites (3DP-ECC): fresh and hardened properties, Cement Concr. Res. 143 (2021), 106388.
[265] H. Ogura, V.N. Nerella, V. Mechtcherine, Developing and testing of strain-hardening cement-based composites (SHCC) in the context of 3D-printing, Materials 11 (8) (2018) 1375.
[266] P. Odaglia, et al., Advances in binder-jet 3D printing of non-cementitious materials, in: RILEM International Conference on Concrete and Digital Fabrication, Springer, 2020.
[267] V. Voney, et al., Powder bed 3D printing with quarry waste, in: IOP Conference Series: Earth and Environmental Science, IOP Publishing, 2020.
[268] S. Pilehvar, et al., Utilization of urea as an accessible superplasticizer on the moon for lunar geopolymer mixtures, J. Clean. Prod. 247 (2020), 119177.
[269] O. Ly, et al., Optimisation of 3D printed concrete for artificial reefs: biofouling and mechanical analysis, Construct. Build. Mater. 272 (2021), 121649.
[270] D.L. Kong, J.G. Sanjayan, Damage behavior of geopolymer composites exposed to elevated temperatures, Cement Concr. Compos. 30 (10) (2008) 986–991.
[271] C.K. Yip, et al., Effect of calcium silicate sources on geopolymerisation, Cement Concr. Res. 38 (4) (2008) 554–564.
[272] S.H. Bong, et al., Fresh and hardened properties of 3D printable geopolymer cured in ambient temperature, in: RILEM International Conference on Concrete and Digital Fabrication, Springer, 2018.
[273] S.H. Bong, et al., Properties of 3D-printable ductile fibre-reinforced geopolymer composite for digital construction applications, in: Rheology and Processing of Construction Materials, Springer, 2019, pp. 363–372.
[274] J. Archez, et al., Shaping of geopolymer composites by 3D printing, J. Build. Eng. 34 (2021), 101894.
[275] A.U. Rehman, V.M. Sglavo, 3D printing of geopolymer-based concrete for building applications, Rapid Prototyp. J. (2020).
[276] Z. Li, L. Wang, G. Ma, Mechanical improvement of continuous steel microcable reinforced geopolymer composites for 3D printing subjected to different loading conditions, Compos. B Eng. 187 (2020), 107796.
[277] T.-F. Yuan, J.-Y. Lee, Y.-S. Yoon, Enhancing the tensile capacity of no-slump high-strength high-ductility concrete, Cement Concr. Compos. 106 (2020), 103458.
[278] R. Mishra, et al., Modelling and simulation of earthquake resistant 3D woven textile structural concrete composites, Compos. B Eng. 81 (2015) 91–97.
[279] R. Mishra, FEM based prediction of 3D woven fabric reinforced concrete under mechanical load, J. Build. Eng. 18 (2018) 95–106.
[280] D. Asprone, et al., Rethinking reinforcement for digital fabrication with concrete, Cement Concr. Res. 112 (2018) 111–121.
[281] T. Marchment, J. Sanjayan, Mesh reinforcing method for 3D concrete printing, Autom. ConStruct. 109 (2020), 102992.
[282] F. Bester, et al., Reinforcing digitally fabricated concrete: a systems approach review, Addit. Manuf. 37 (2021), 101737.
[283] F. Bos, E. Bosco, T. Salet, Ductility of 3D printed concrete reinforced with short straight steel fibers, Virtual Phys. Prototyp. 14 (2) (2019) 160–174.
[284] B. Nematollahi, et al., Effect of type of fiber on inter-layer bond and flexural strengths of extrusion-based 3D printed geopolymer, in: Materials Science Forum, Trans Tech Publ, 2018.
[285] N. Hack, H. Kloft, Shotcrete 3D printing technology for the fabrication of slender fully reinforced freeform concrete elements with high surface quality: a real-scale demonstrator, in: RILEM International Conference on Concrete and Digital Fabrication, Springer, 2020.
[286] N. Taha, et al., Robotic AeroCrete–A novel robotic spraying and surface treatment technology for the production of slender reinforced concrete elements, in: Architecture in the Age of the 4th Industrial Revolution–Proceedings of the 37th eCAADe and 23rd SIGraDi Conference, CumInCAD, 2019.
[287] K. Korniejenko, et al., Mechanical properties of short fiber-reinforced geopolymers made by casted and 3D printing methods: a comparative study, Materials 13 (3) (2020) 579.
[288] M.H. Raza, R.Y. Zhong, M. Khan, Recent Advances and Productivity Analysis of 3D Printed Geopolymers, Addit. Manuf. (2022), 102685.
[289] S.Z. Jones, et al., 3D Printing Using Concrete Extrusion: a Roadmap for Research, 2018.
[290] B. Panda, et al., Current challenges and future potential of 3D concrete printing: aktuelle Herausforderungen und Zukunftspotenziale des 3D-Druckens bei Beton, Mater. Werkst. 49 (5) (2018) 666–673.
[291] P. Carneau, et al., Additive manufacturing of cantilever - from masonry to concrete 3D printing, Autom. ConStruct. 116 (2020), 103184.
[292] V. Mechtcherine, et al., A roadmap for quality control of hardening and hardened printed concrete, Cement Concr. Res. 157 (2022), 106800.
[293] X. Li, Z. Wang, Z. Jiao, Influence of curing on the strength development of calcium-containing geopolymer mortar, Materials 6 (11) (2013) 5069–5076.
[294] Y.-S. Wang, Y. Alrefaei, J.-G. Dai, Influence of coal fly ash on the early performance enhancement and formation mechanisms of silico-aluminophosphate geopolymer, Cement Concr. Res. 127 (2020), 105932.
[295] H.U. Ahmed, A.A. Mohammed, A. Mohammad, The role of nanomaterials in geopolymer concrete composites: a state-of-the-art review, J. Build. Eng. (2022), 104062.
[296] S.M. Qaidi, et al., Recycling of mine tailings for the geopolymers production: a systematic review, Case Stud. Constr. Mater. (2022), e00933.